

## Supplementary materials

# New anticandidal Cu(I) complexes with neocuproine and ketoconazole derived diphenyl(aminomethyl)phosphane: luminescence properties for detection in fungal cells. †

Radosław Starosta,<sup>a,b,\*</sup> Rodrigo F. M. de Almeida,<sup>b</sup> Małgorzata Puchalska,<sup>a</sup> Agata Białońska,<sup>a</sup> Jarosław J. Panek,<sup>a</sup> Aneta Jezierska,<sup>a</sup> Ida Szmigiel,<sup>c</sup> Jakub Suchodolski<sup>c</sup> and Anna Krasowska<sup>c</sup>

<sup>a</sup> Faculty of Chemistry, University of Wrocław, F. Joliot-Curie 14, 50-383 Wrocław, Poland.

<sup>b</sup> Centro de Química Estrutural, Faculdade de Ciências da Universidade de Lisboa, Campo Grande, 1749-016 Lisboa, Portugal

<sup>c</sup> Faculty of Biotechnology, University of Wrocław, F. Joliot-Curie 14a, 50-383 Wrocław, Poland

\* e-mail: radoslaw.starosta@chem.uni.wroc.pl

## Abstract

The search for new antifungals is very important because the large genetic variation of pathogenic organisms has resulted in the development of increasingly effective defense mechanisms by microorganisms. Metal complexes as potential drugs are gaining nowadays an interest, because they are characterized by accessible redox states of metal centers and plethora of easily modifiable geometries. In this work we present two new copper(I) iodide or thiocyanide complexes with 2,9-dimethyl-1,10-phenanthroline (dmp) and diphenylphosphane derivative of ketoconazole (**KeP**), where ketoconazole acetyl group is replaced by -CH<sub>2</sub>PPh<sub>2</sub> unit, [Cu(dmp)KeP] (**1-KeP**) and [CuNCS(dmp)KeP] (**2-KeP**) - their synthesis and structural characteristics. The analysis of the intrinsic fluorescence of ketoconazole moiety in the coordinated **KeP** molecule revealed that the copper(I) central atom does not act as a quencher and the observed decrease of fluorescence intensity is a result of a strong inner filter effect caused by the presence of CuXdmp unit. Moreover, the complexes exhibit a remarkable MLCT (metal - ligand charge transfer) based phosphorescence with the emission maximum at 600-615 nm in aqueous media, which probably results from the formation of dimers and higher order oligomers in the most polar solutions. Both complexes proved to be promising antifungal agents towards *Candida albicans*, showing a relatively high efficiency towards the fluconazole resistant strains with - *CDR1* and *CDR2* or *MDR1* efflux pumps overexpression, what suggests that they overcome at least partially these defense mechanisms. Simulations of docking to the cytochrome P450 14 $\alpha$ -demethylase (the azoles' primary molecular target) suggested that the compounds studied were rather incapable to competitively inhibit this enzyme, unlike ketoconazole and the **KeP** ligand. On the other hand, the phosphorescence in aqueous solutions allowed to record the confocal micrographs of the complexes which showed that both of them are situated in spherical structures inside the cells, most likely in the vacuoles.

## Table of contents:

1. **Fig.S1.** Molecular scheme of **KeP** with atoms numbering for the NMR data.
2. **Fig.S2.** Molecular scheme of the studied complexes with atoms numbering for the NMR data.
3. **Tab.S1.** Chemical shifts and coupling constants from the <sup>13</sup>C{<sup>1</sup>H} NMR spectra of **Ke**, **KeOP** (from ref. [580]), **1-KeP** and **2-KeP** in CDCl<sub>3</sub>.
4. **Tab.S2.** Chemical shifts and coupling constants from the <sup>31</sup>P{<sup>1</sup>H} and <sup>1</sup>H NMR spectra of **Ke**, **KeOP** (from ref. [5150]), **1-KeP** and **2-KeP** in CDCl<sub>3</sub>.
5. **Fig. S3.** <sup>31</sup>P{<sup>1</sup>H} and <sup>1</sup>H NMR spectra of **1-KeP** in CDCl<sub>3</sub>. (T = 300K).
6. **Fig. S4.** <sup>13</sup>C{<sup>1</sup>H} NMR spectra of **1-KeP** in CDCl<sub>3</sub>. (T = 300K).
7. **Fig.S5.** 2D <sup>1</sup>H-<sup>13</sup>C HMQC NMR spectra of **1-KeP** in CDCl<sub>3</sub>. (T = 300K).
8. **Fig. S6.** <sup>1</sup>H and <sup>31</sup>P{<sup>1</sup>H} NMR spectra of **2-KeP** in CDCl<sub>3</sub>. (T = 300K).

9. **Fig. S7.**  $^{13}\text{C}\{^1\text{H}\}$  NMR spectra of **2-KeP** in  $\text{CDCl}_3$ . (T = 300K).
10. **Fig.S8.** Normalized solid state luminescence (upon the excitation at 380 nm; right) and excitation (for the emission at the band maximum; left) spectra of the studied complexes studied at room temperature (r.t. - dashed red lines) and at 77K (solid lines).
11. **Tab.S3** Spectroscopic data for the studied compounds in organic solvents.
12. **Fig.S9.** Absorption, normalized excitation (for the emission at 370 nm) and emission spectra (for the excitation at 295 nm) for the complexes and organic compounds (c = 100 $\mu\text{M}$ ) in four different solvents.
13. **Fig.S10.** Luminescence data for **1-KeP** in  $\text{H}_2\text{O}+\text{DMSO}$  (A, B) and  $\text{H}_2\text{O}+\text{CH}_3\text{CN}$  (C, D) in two concentrations: 100  $\mu\text{M}$  (•black squares) and 20  $\mu\text{M}$  (•red circles). A, C: fluorescence intensity at the band maximum (excitation: 295 nm) B, D: position of the fluorescence band maximum (excitation: 295 nm) as function of the mole fraction of the organic solvent (DMSO or  $\text{CH}_3\text{CN}$ ).
14. **Fig.S11-A-C.** Staining of the DSY1050 strain with **1-KeP** imaged by confocal microscopy (excitation at 405 nm, emission 600 - 700 nm signal collected). Top: bright field; Middle: luminescence; Bottom: merged.
15. **Fig.S12-A-B.** Staining of the DSY1050 strain with **2-KeP** imaged by confocal microscopy (excitation at 405 nm, emission 600 - 700 nm signal collected). Top: bright field; Middle: luminescence; Bottom: merged.
16. **Fig.S13** Proliferation rate of NHDF cells measured by MTT assay. NHDF cells were treated with 0.25; 0.5; 1; 2 and 4 x  $\text{MIC}_{50}$  concentrations of Ke, Flc and 1-KeP for 72 h, incubated with MTT and the number of viable cells measured spectrophotometrically at 540 nm. The bars represent the means  $\pm$  SD of triplicate values for three independent experiments. \*\*\*P<0.001.
17. **Fig.S14** Docking of a) **1-KeP** (orange) and b) **2-KeP** (purple) to the CYP51 of *C. albicans* (grey ribbons). Experimental positions of the heme cofactor (pink) and the inhibitor – posaconazole (cyan) – are taken from the 5FSA PDB deposit. Docking ensembles of 27 conformations are shown for each ligand. The large molecules of the complexes **1-KeP** and **2-KeP** are not able to enter the binding cavity accessible to the posaconazole molecule; in particular, they are not able to interact directly with the heme cofactor. They are, instead, located on the protein surface, possibly obstructing the entrance to the binding cavity.
18. References –extended information on the cited papers in the main article.

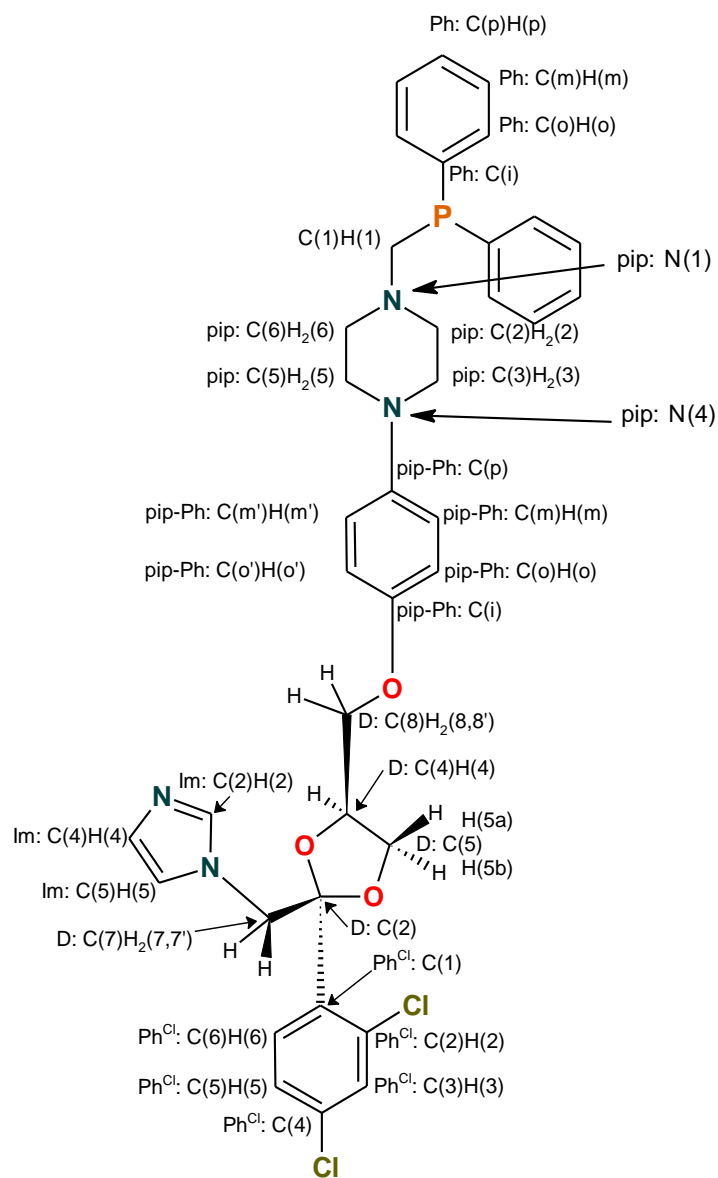


**Fig.S1.** Molecular scheme of **KeP** with atoms numbering for the NMR data.

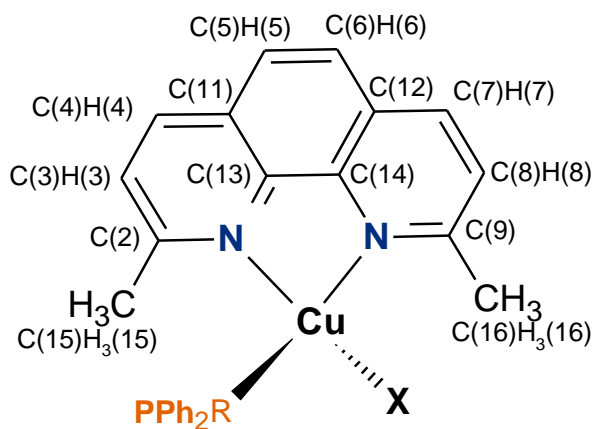


**Fig.S2.** Molecular scheme of the studied complexes with atoms numbering for the NMR data.

**Tab.S1.** Chemical shifts and coupling constants from the  $^{13}\text{C}\{^1\text{H}\}$  NMR spectra of **KeP**, **KeOP**, **1-KeP** and **2-KeP** in  $\text{CDCl}_3$ .

	$^{13}\text{C}\{^1\text{H}\}$	<b>KeP</b> *		<b>KeOP</b> *		<b>1-KeP</b>		<b>2-KeP</b>		dmp
-CH <sub>2</sub> PPh <sub>2</sub>	C(1) d	61.40	3.6	58.43	88.1	59.08	27.2	59.16	26.3	
	C(i) d	138.38	12.7	132.42	97.2	not obs.		134.87	25.4	
	C(o) d	132.83	18.2	131.28	9.1	133.06	12.7	132.64	13.6	
	C(m) d	128.36	6.4	128.50	11.8	128.23	8.2	128.37	8.2	
	C(p) s/d	128.52	-	131.86	2.7	129.30		129.36		
pip	C(2;6) d	54.55	9.1	55.54	8.2	55.23	5.4	55.07	6.4	
	C(3,5) s	50.46		50.43		49.94		50.07		
pip-Ph	C(i) s	152.19		152.28		152.01		152.15		
	C(o) s	117.99		117.98		117.62		117.77		
	C(m) s	115.15		115.18		115.06		115.13		
	C(p) s	146.18		146.05		145.89		145.94		
D	C(2) s	107.97		108.00		107.84		107.97		
	C(4) s	74.79		74.81		74.74		74.80		
	C(5) s	67.71		67.75		67.68		67.74		
	C(7) s	51.27		51.31		51.30		51.32		
	C(8) s	67.57		67.60		67.53		67.59		
Im	C(2) s	131.30		131.35		131.28		131.33		
	C(4) s	127.17		127.21		127.17		127.21		
	C(5) s	129.48		129.51		129.48		129.51		
PhCl	C(1) s	135.80		135.85		135.80		135.84		
	C(2) s	134.60		134.61		134.47		134.59		
	C(3) s	138.74		138.78		139.01		139**	s**	
	C(4) s	132.94		132.98		132.90		132.96		
	C(5) s	128.55		128.56		128.44		128.5*	s*	
	C(6) s	121.07		121.12		121.16		121.2*	s*	
dmp	C <sup>2,9</sup> s					159.28		158.96		159.07
	C <sup>3,8</sup> s					124.81		124.88		123.29
	C <sup>4,7</sup> s					136.35		136.47		136.07
	C <sup>5,6</sup> s					125.28		125.36		125.22
	C <sup>11,12</sup> s					142.98		142.93		145.03
	C <sup>13,14</sup> s					126.96		126.91		126.58
	CH <sub>3</sub> s					26.76		26.36		26.64

\* - data from de Almeida R.F.M., Santos F.C., Marycz K., Alicka M., Krasowska A., Suchodolski J., Panek J.J., Jezierska A., Starosta R., New diphenylphosphane derivatives of ketoconazole are promising antifungal agents. Sci. Rep. 2019, 9, 16214 <https://doi.org/10.1038/s41598-019-52525-7>

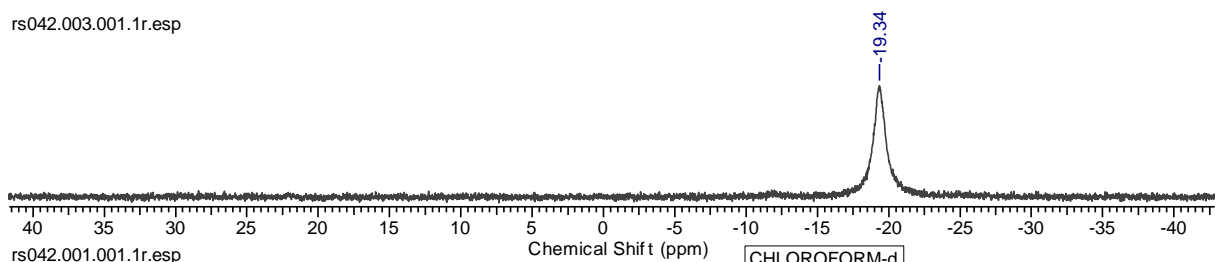
**Tab.S2.** Chemical shifts and coupling constants from the  $^{31}\text{P}\{^1\text{H}\}$  and  $^1\text{H}$  NMR spectra of **KeP**, **KeOP**, **1-KeP** and **2-KeP** in  $\text{CDCl}_3$ .

		<b>KeP *</b>			<b>KeOP *</b>			<b>1-KeP</b>			<b>2-KeP</b>
$^{31}\text{P}\{^1\text{H}\}$		-27.39			27.18			-19.3*			-18.6*
$^1\text{H}$ NMR:											
-CH <sub>2</sub> PPh <sub>2</sub>	H(1) d	3.28	2.9	3.31	6.9	3.51*		3.30*			
	Ph	7.32-7.38 7.47-7.50	6H 4H	7.46-7.55 7.83-7.87	6H 4H	7.22-7.32 7.60-7.63	6H 4H	7.22-7.32 7.41-7.44	6H 4H		
pip	H(2;6) m	2.83		2.81		2.54		2.50			
	H(3,5) m	3.12		3.03		2.66		2.70			
pip-Ph	H(o) AA'	6.89		6.84		6.69		6.71	(one		
	H(m) BB'	6.75		6.73		6.67		6.71	singlet)		
D	H(4) dddd	4.34	6.6; 6.5; 5.1; 5.0	4.34	6.6; 6.5; 5.1; 5.0	4.32	6.6; 6.5; 5.1; 5.0	4.34	6.5; 6.5; 5.1; 5.0		
	H(5a) dd	3.74	8.4; 4.9	3.73	8.4, 4.9	3.71	8.3; 4.9	3.73	8.4; 4.9		
	H(5b) dd	3.88	8.3; 6.6	3.87	8.4; 6.5	3.86	8.5; 6.6	3.88	8.3; 6.6		
	H(7) A	4.51	14.68	4.51	14.88	4.49	14.7	4.51	14.7		
	H(7') B	4.41	14.68	4.42	14.88	4+3.9	14.7	4.49	14.7		
	H(8) dd	3.74	9.7; 5.1	3.74	9.6, 5.1	3.71	9.9; 5.1	3.73	9.6; 5.2		
	H(8') dd	3.33	9.6; 6.7	3.32	9.6, 6.8	3.30	9.6; 6.8	3.33	9.7; 6.9		
	Im	H(2) d	under Ph		under Ph		7.46	1.9	7.47	1.9	
H(4) dd		7.25	8.4; 2.1	7.25	8.4; 2.2	7.25	8.4; 1.9	under Ph			
H(5) d		7.58	8.4	7.58	8.4	7.57	8.4	7.58	8.4		
PhCl	H(3) s*	7.00		6.99		6.97		6.99			
	H(5) s*	6.97		6.96		6.95		6.97			
	H(6) s*	7.51		under Ph		7.56		7.52			
dmp#	H <sup>5,6</sup> s					7.75		7.76			
	H <sup>4,7</sup> d					8.18	8.2	8.20	8.0		
	H <sup>3,8</sup> d					7.47	8.2	7.51	~8		
	CH <sub>3</sub> s					2.82		2.79			

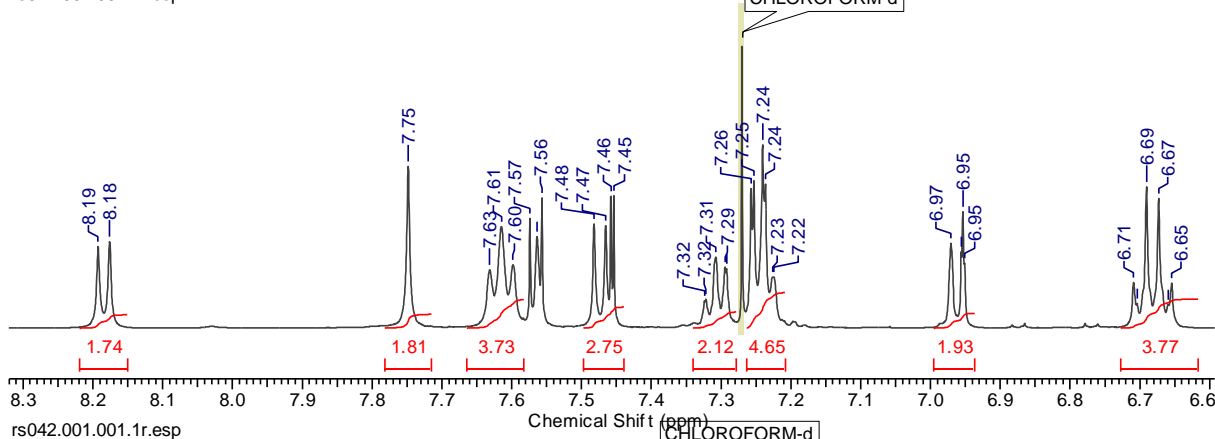
# - Free dmp ligand:  $^1\text{H}$  NMR H<sup>5,6</sup> s: 7.62 ppm; H<sup>4,7</sup>d: 8.04 ppm d (J=8.2 Hz); H<sup>3,8</sup>d: 7.42 ppm (J=8.2 Hz); CH<sub>3</sub> s: 2.90 ppm;

\* - **data from** de Almeida R.F.M., Santos F.C., Marycz K., Alicka M., Krasowska A., Suchodolski J., Panek J.J., Jezierska A., Starosta R., New diphenylphosphane derivatives of ketoconazole are promising antifungal agents. Sci. Rep. 2019, 9, 16214 <https://doi.org/10.1038/s41598-019-52525-7>

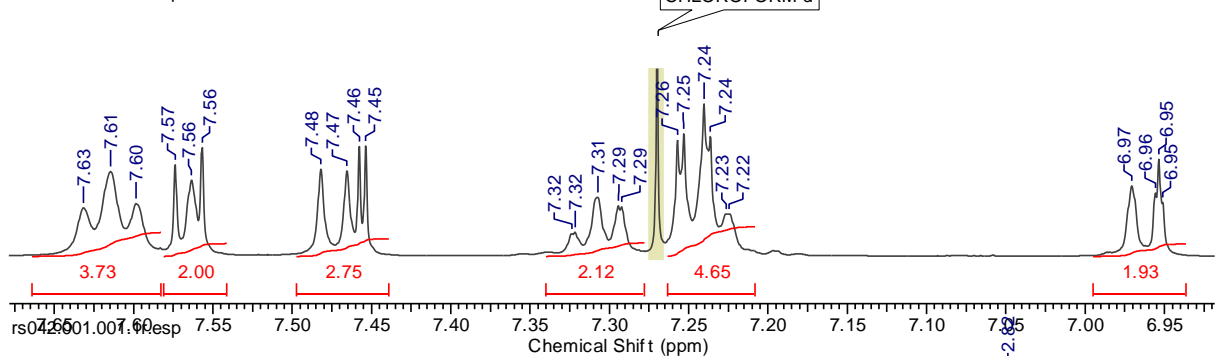
rs042.003.001.1r.esp



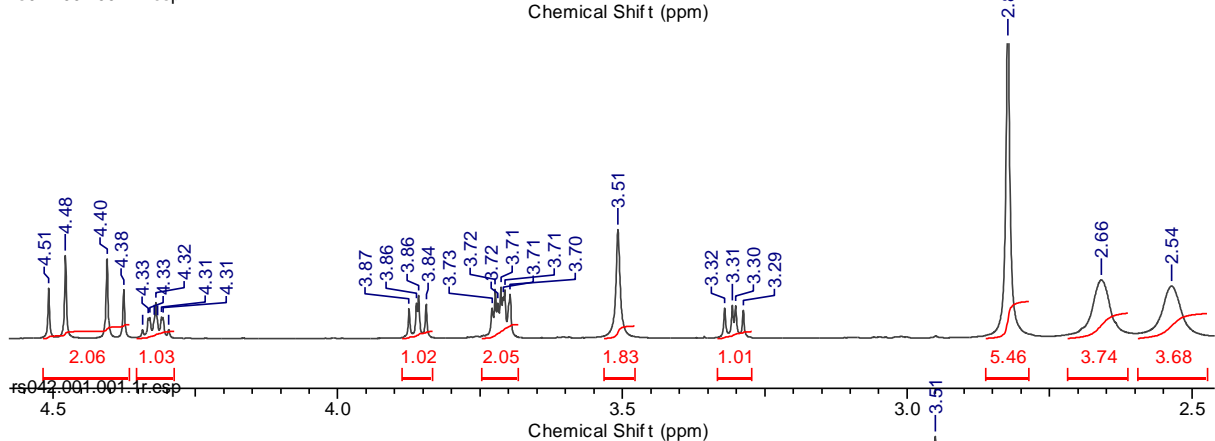
rs042.001.001.1r.esp



rs042.001.001.1r.esp



rs042.001.001.1r.esp



rs042.001.001.1r.esp

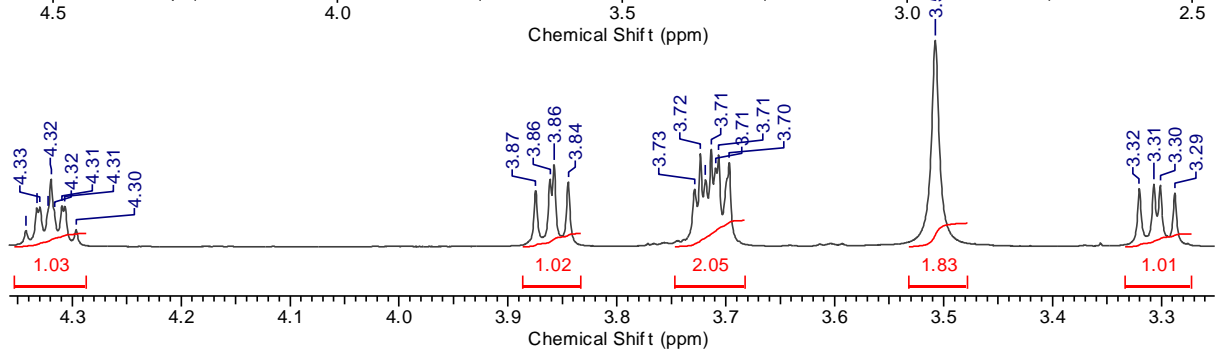
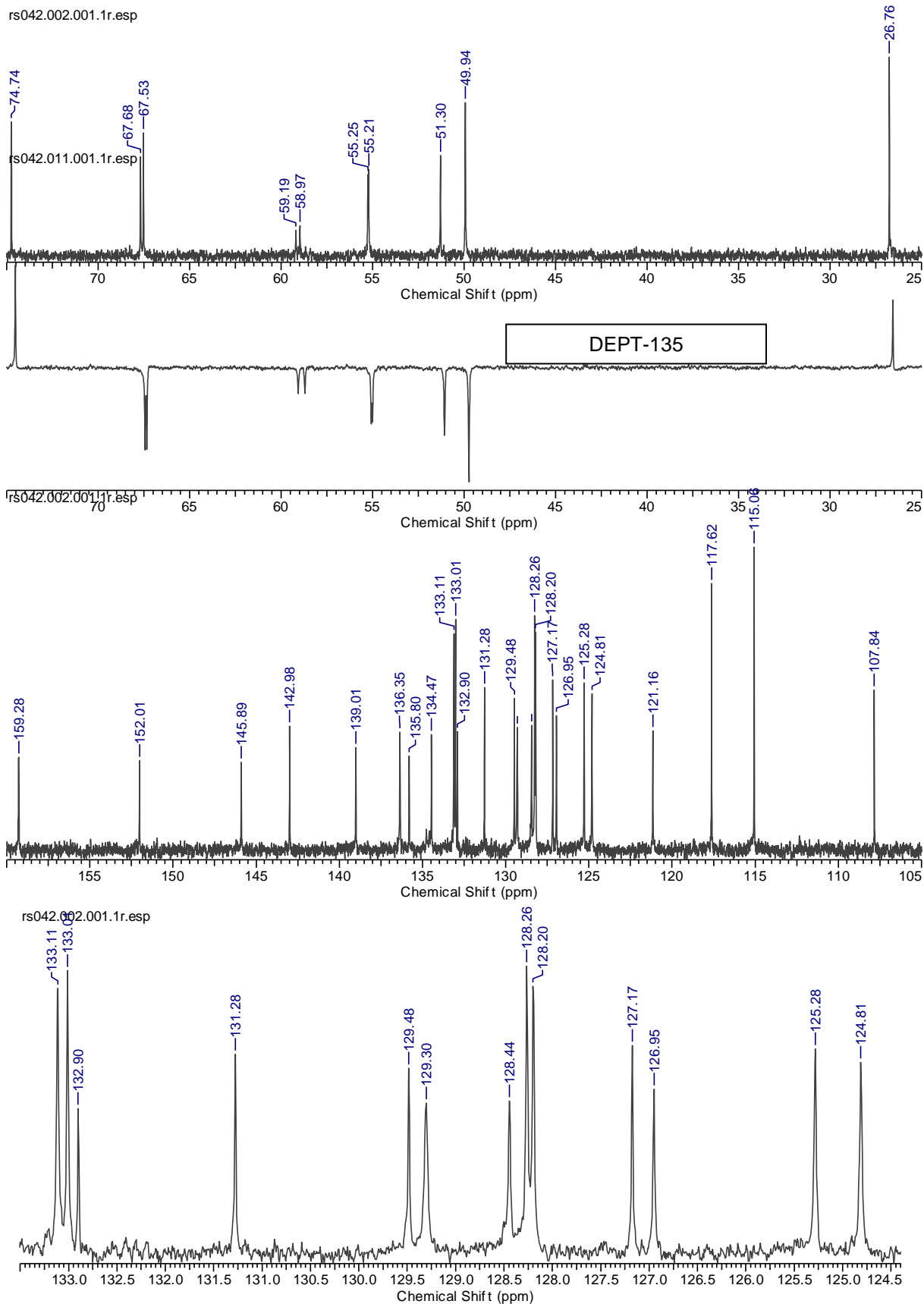
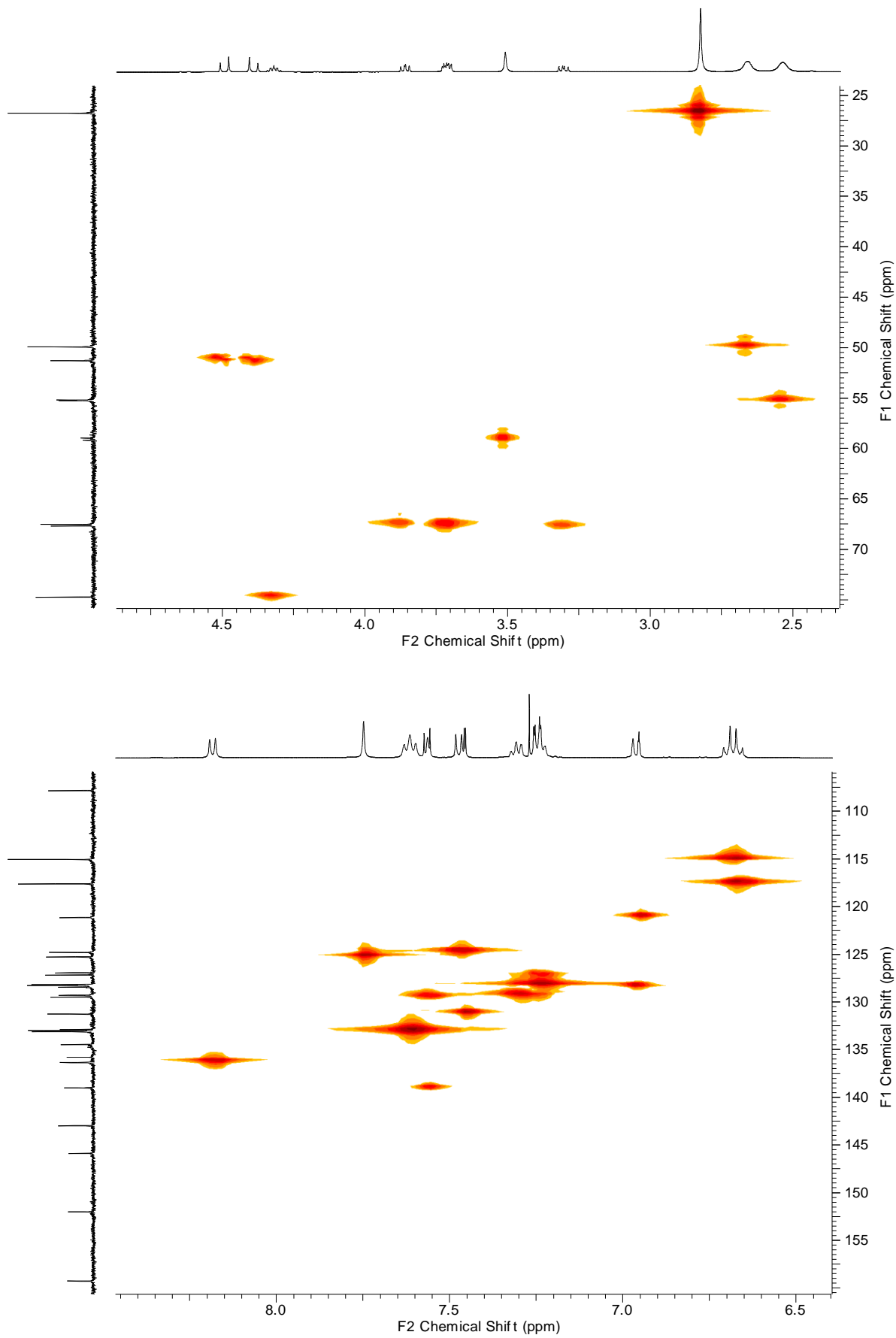


Fig. S3.  $^{31}\text{P}\{^1\text{H}\}$  and  $^1\text{H}$  NMR spectra of **1-KeP** in  $\text{CDCl}_3$ . (T = 300K)



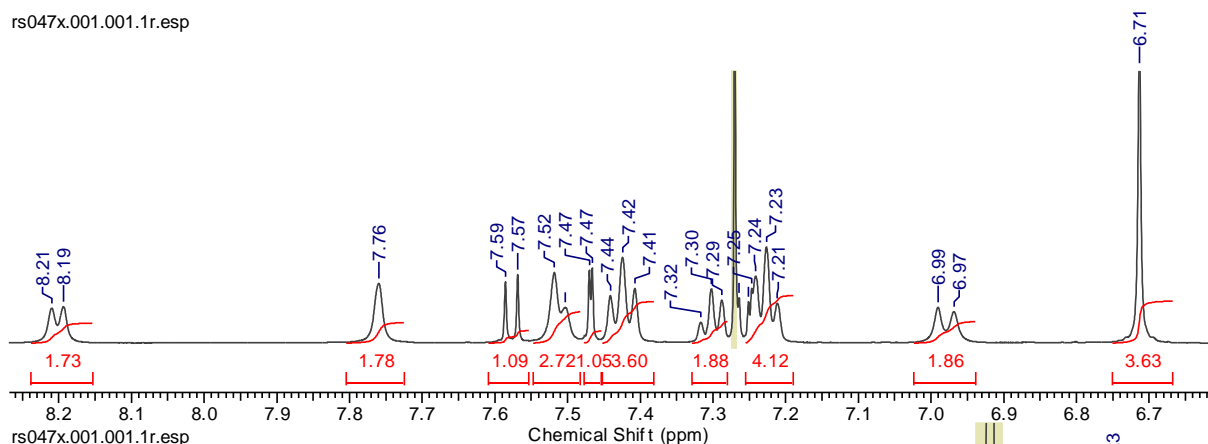
**Fig. S4.**  $^{13}\text{C}\{^1\text{H}\}$  NMR spectra of **1-KeP** in  $\text{CDCl}_3$ . ( $T = 300\text{K}$ )



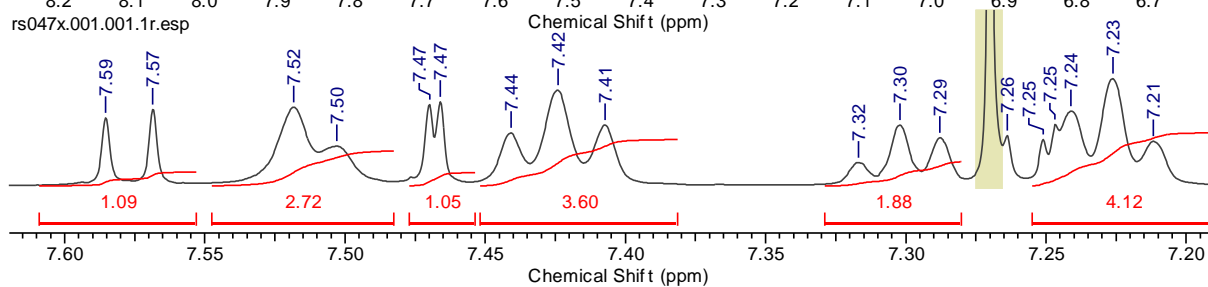
**Fig.S5.** 2D  $^1\text{H}$ - $^{13}\text{C}$  HMQC NMR spectra of **1-KeP** in  $\text{CDCl}_3$ . ( $T = 300\text{K}$ )



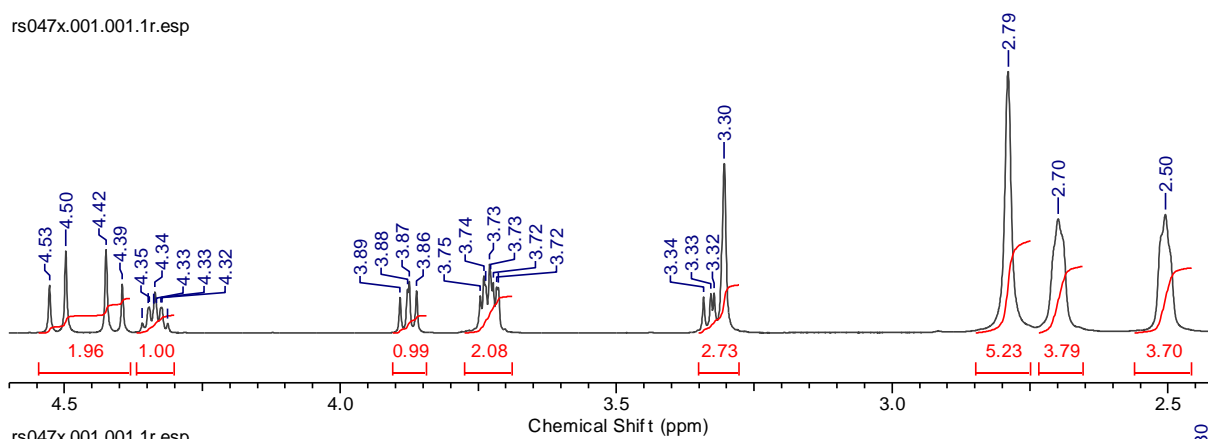
rs047x.001.001.1r.esp



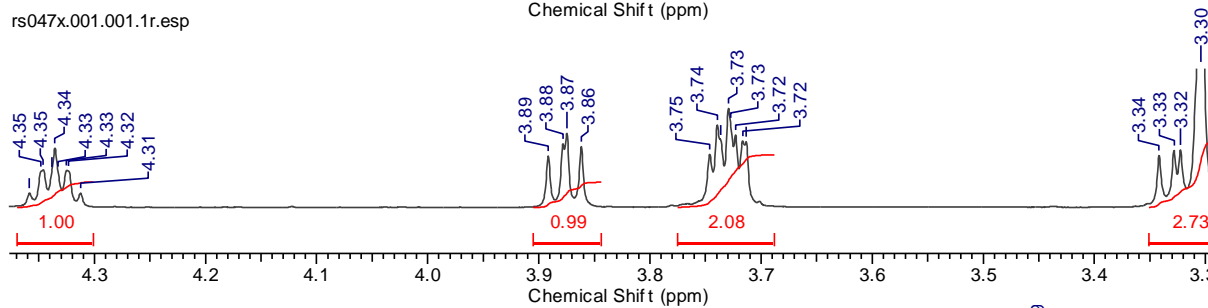
rs047x.001.001.1r.esp



rs047x.001.001.1r.esp



rs047x.001.001.1r.esp



rs047x.005.001.1r.esp

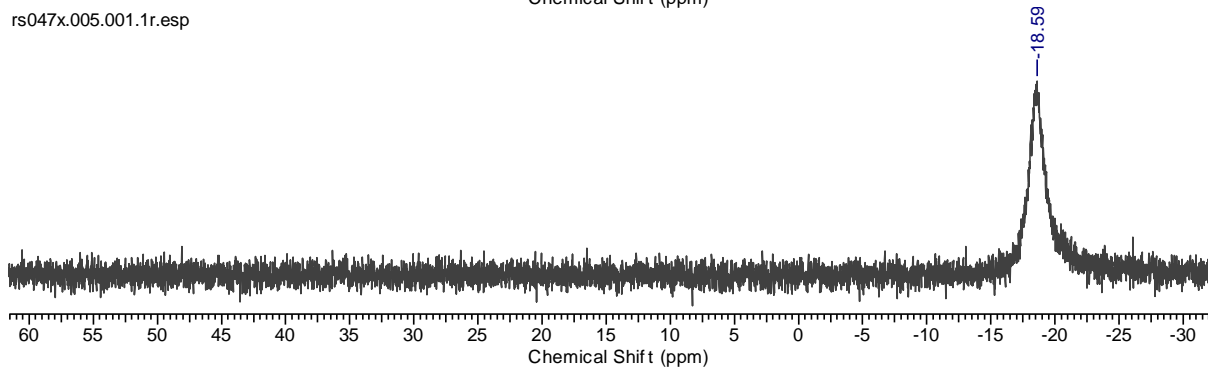
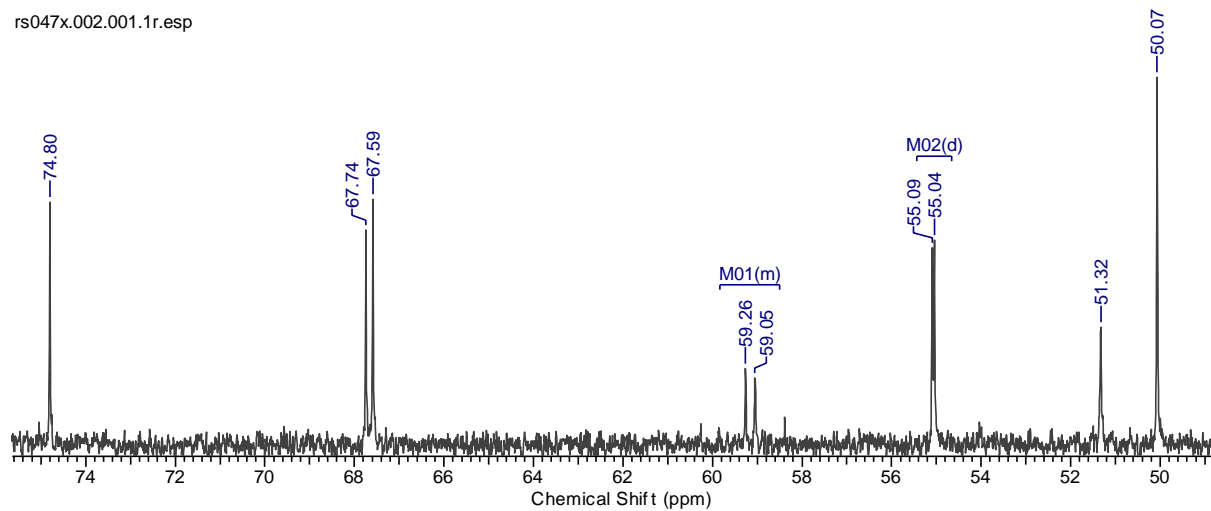
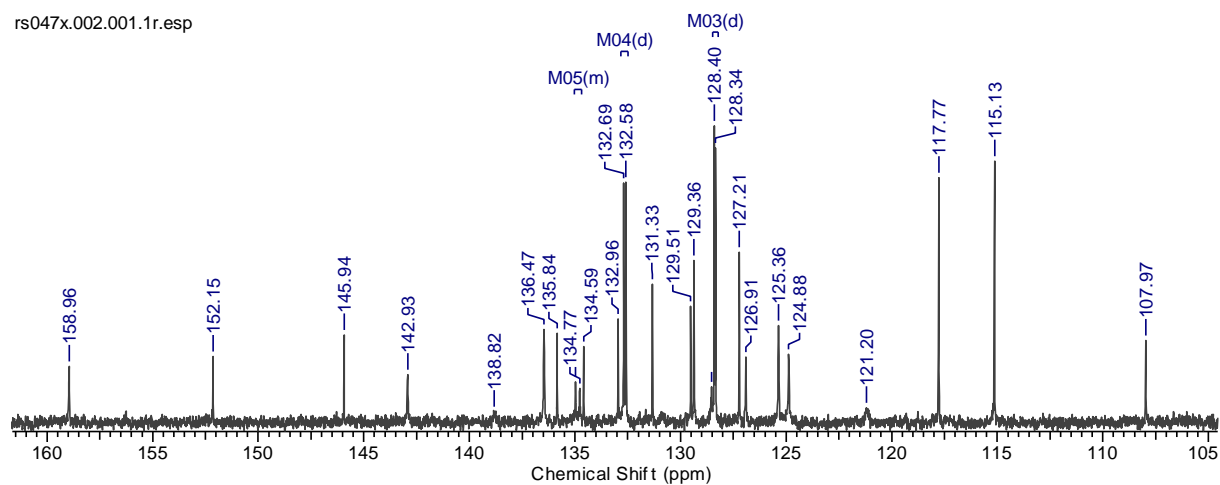


Fig. S6.  $^1\text{H}$  and  $^{31}\text{P}\{^1\text{H}\}$  NMR spectra of 2-KeP in  $\text{CDCl}_3$ . (T = 300K)

rs047x.002.001.1r.esp



rs047x.002.001.1r.esp



rs047x.002.001.1r.esp

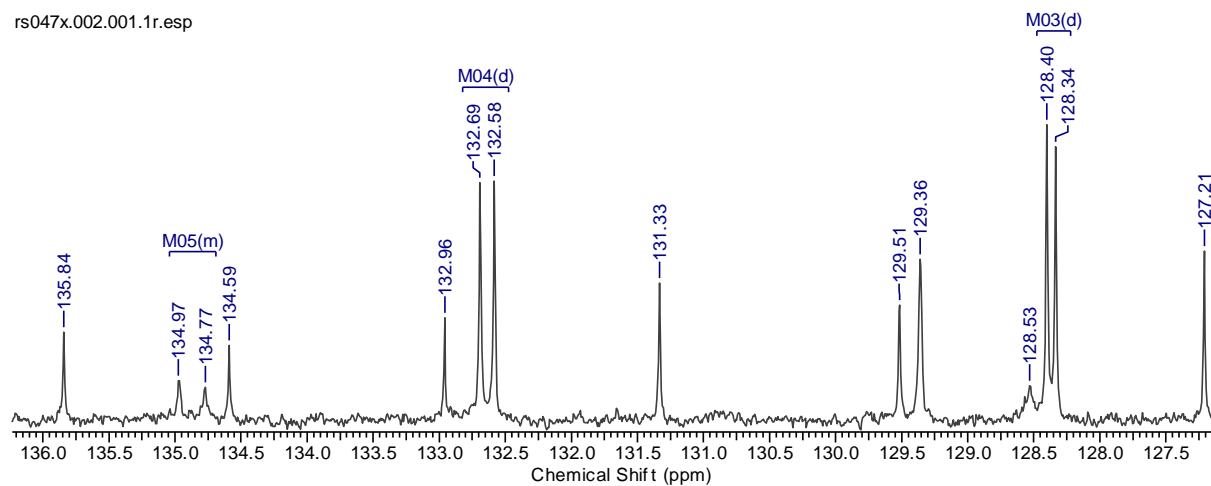
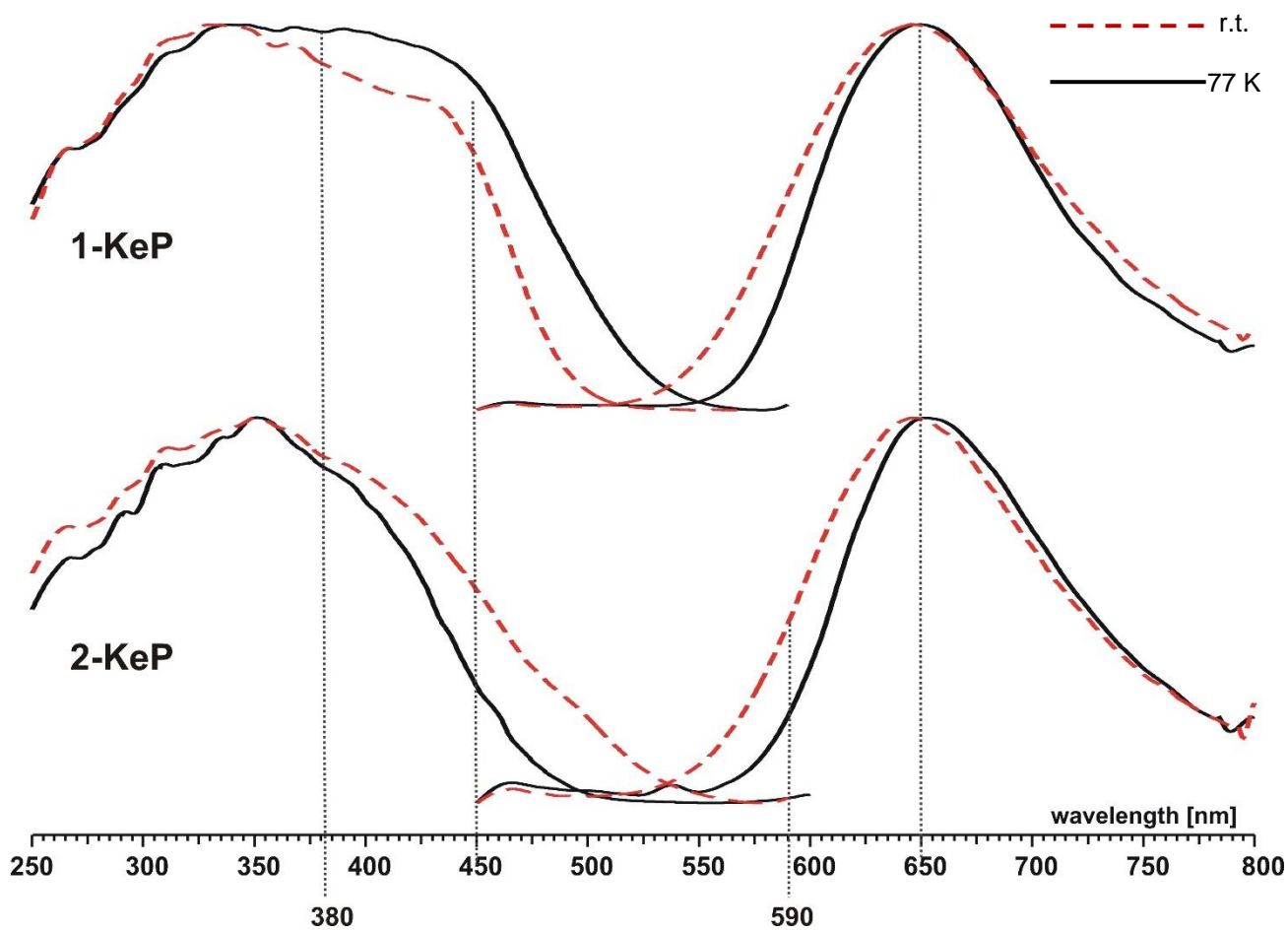


Fig. S7. <sup>13</sup>C{<sup>1</sup>H} NMR spectra of 2-KeP in CDCl<sub>3</sub>. (T = 300K)



**Fig.S8.** Normalized solid state luminescence (upon the excitation at 380 nm; right) and excitation (for the emission at the band maximum; left) spectra of the studied complexes studied at room temperature (r.t. - dashed red lines) and at 77K (solid lines).

**Tab.S3** Spectroscopic data for the compounds in organic solvents

	Ke	KeP	KeOP	1-KeP	2-KeP
MeOH					
ABS: $\lambda_{\max}$	1: 297 * 2: 243 *	1: <i>sh</i> * 2: 246 *	1: 299* 2: 243 *		
EM <sup>(295)</sup> $\lambda_{\max}$	368 *	373 *	369 *	362	361
EX <sup>(370)</sup> $\lambda_{\max}$	293 *	297 *	295 *	289 <sup>sh</sup> ,302#	289 <sup>sh</sup> ,302#
LT: (280→370) $\tau$ /ns (a) [ $\chi^2$ ]	1: 0.28 (0.087) * 2: 1.63 (0.913) * [1.525] * <b>&lt;<math>\tau</math>&gt;: 1.51 *</b>	0.11 (0.464) * 1.37 (0.536) * [1.434] * <b>&lt;<math>\tau</math>&gt;: 0.78 *</b>	0.29 (0.506) * 0.58 (0.494) * [1.446] * <b>&lt;<math>\tau</math>&gt;: 0.43 *</b>	1.43 (0.964) 2.66 (0.036) [1.225] <b>&lt;<math>\tau</math>&gt;: 1.47</b>	1.34 (0.866) 2.08 (0.536) [1.321] <b>&lt;<math>\tau</math>&gt;: 1.44</b>
EtOH					
ABS: $\lambda_{\max}$	1: 295 * 2: 245 *	1: <i>sh</i> * 2: 247 *	1: 295 * 2: 245 *		
EM <sup>(295)</sup> $\lambda_{\max}$	362 *	365 *	363 *	368	369
EX <sup>(370)</sup> $\lambda_{\max}$	291 *	296 *	295 *	291 <sup>sh</sup> ,303#	291 <sup>sh</sup> ,302#
LT: (280→370) $\tau$ /ns (a) [ $\chi^2$ ]	1: 1.05 (0.209) 2: 1.68 (0.791) [1.283] <b>&lt;<math>\tau</math>&gt;: 1.55</b>	1: 0.62 (0.233) 2: 1.37 (0.767) [1.509] <b>&lt;<math>\tau</math>&gt;: 1.19</b>	1: 0.46 (0.981) 2: 1.95 (0.019) [1.362] <b>&lt;<math>\tau</math>&gt;: 0.49</b>	1: 0.50 (0.513) 2: 1.57 (0.487) [2.131] <b>&lt;<math>\tau</math>&gt;: 1.02</b>	1: 0.49 (0.521) 2: 1.52 (0.479.) [2.185] <b>&lt;<math>\tau</math>&gt;: 0.98</b>
CH <sub>3</sub> CN					
ABS: $\lambda_{\max}$	1: 299 * 2: 247 *	1: <i>sh</i> * 2: 250 *	1: 305 * 2: 249 *		
EM <sup>(295)</sup> $\lambda_{\max}$	370 *	372 *	372 *	371	373
EX <sup>(370)</sup> $\lambda_{\max}$	301 *	306 *	303 *	291 <sup>sh</sup> ,306#	291 <sup>sh</sup> ,306#
LT: (280→370) $\tau$ /ns (a) [ $\chi^2$ ]	1: 1.22 (0.355) 2: 1.71 (0.645) [1.051] <b>&lt;<math>\tau</math>&gt;: 1.53</b>	1: 1.13 (0.779) 2: 1.62 (0.221) [1.189] <b>&lt;<math>\tau</math>&gt;: 1.24</b>	1: 0.85 (0.979) 2: 2.10 (0.021) [1.277] <b>&lt;<math>\tau</math>&gt;: 0.88</b>	1: 0.67 (0.463) 2: 1.47 (0.537) [1.343] <b>&lt;<math>\tau</math>&gt;: 1.10</b>	1: 0.59 (0.413) 2: 1.45 (0.587) [1.203] <b>&lt;<math>\tau</math>&gt;: 1.09</b>
DMSO					
ABS: $\lambda_{\max}$	303	<i>sh</i>	306		
EM <sup>(295)</sup> $\lambda_{\max}$	374	374	377	378	377
EX <sup>(370)</sup> $\lambda_{\max}$	300	307	305	291 <sup>sh</sup> ,311#	291 <sup>sh</sup> ,310#
LT: (280→370) $\tau$ /ns (a) [ $\chi^2$ ]	1: 1.33 (0.986) 2: 3.27 (0.014) [1.151] <b>&lt;<math>\tau</math>&gt;: 1.36</b>	1: 1.03 (0.979) 2: 2.44 (0.021) [1.352] <b>&lt;<math>\tau</math>&gt;: 1.06</b>	1: 0.54 (0.995) 2: 4.48 (0.005) [1.544] <b>&lt;<math>\tau</math>&gt;: 0.56</b>	1: 0.99 (0.987) 2: 3.87 (0.013) [1.456] <b>&lt;<math>\tau</math>&gt;: 1.03</b>	1: 1.02 (0.987) 2: 3.86 (0.015) [1.572] <b>&lt;<math>\tau</math>&gt;: 1.06</b>

*sh* – shoulder; # inner-filter effect; **< $\tau$ >** =  $\tau_{1a1} + \tau_{2a2}$  [ns]; \* - data from: Starosta R., de Almeida R.F.M. "Luminescence properties of the antifungal agent ketoconazole and its diphenylphosphane derivatives" J. Lumin. 2020, 220, 116956; DOI: 10.1016/j.jlumin.2019.116956

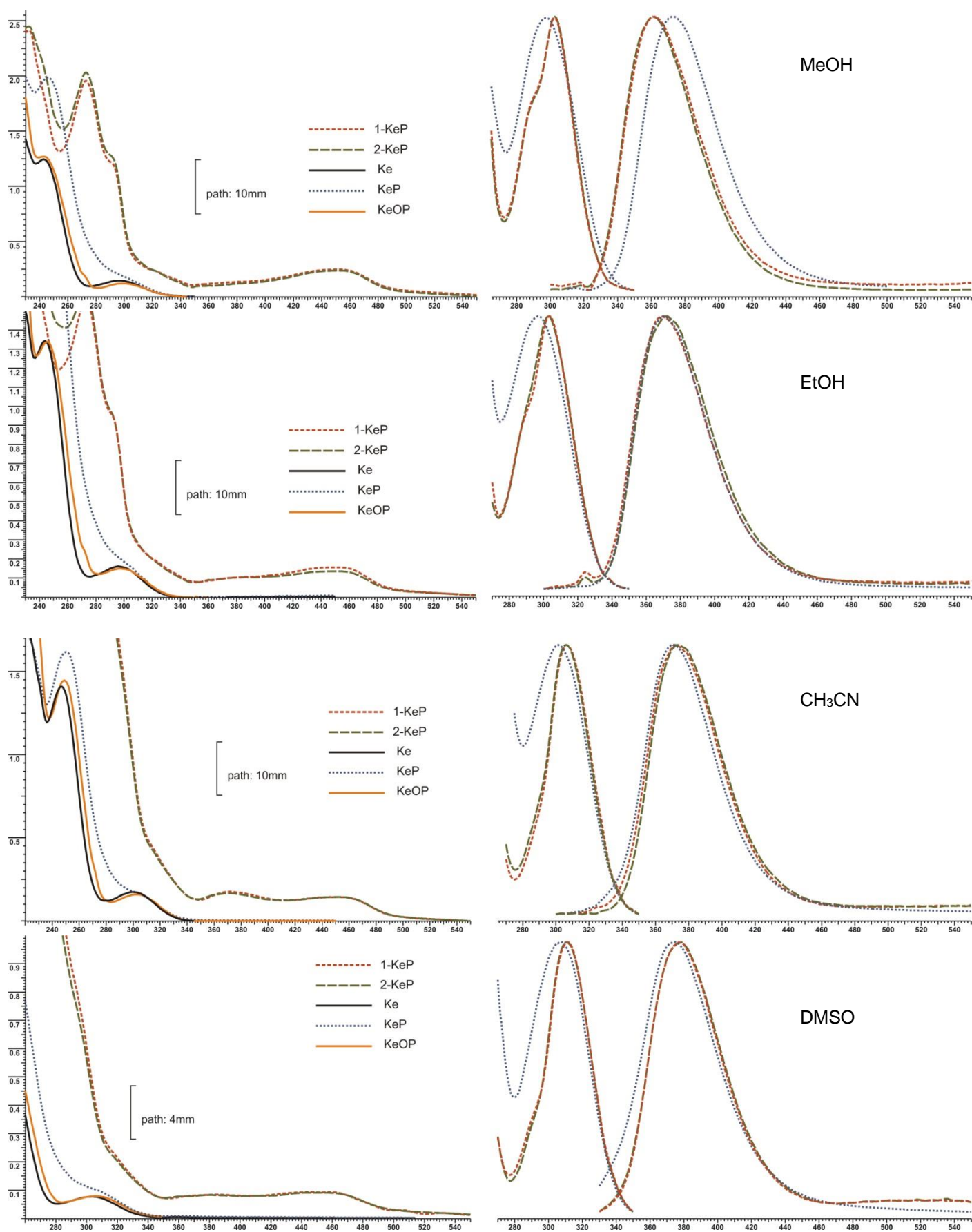


**Fig.S9.** Absorption, normalized excitation (for the emission at 370 nm) and emission spectra (for the excitation at 295 nm) for the complexes and organic compounds (c = 100  $\mu$ M) in four different solvents.

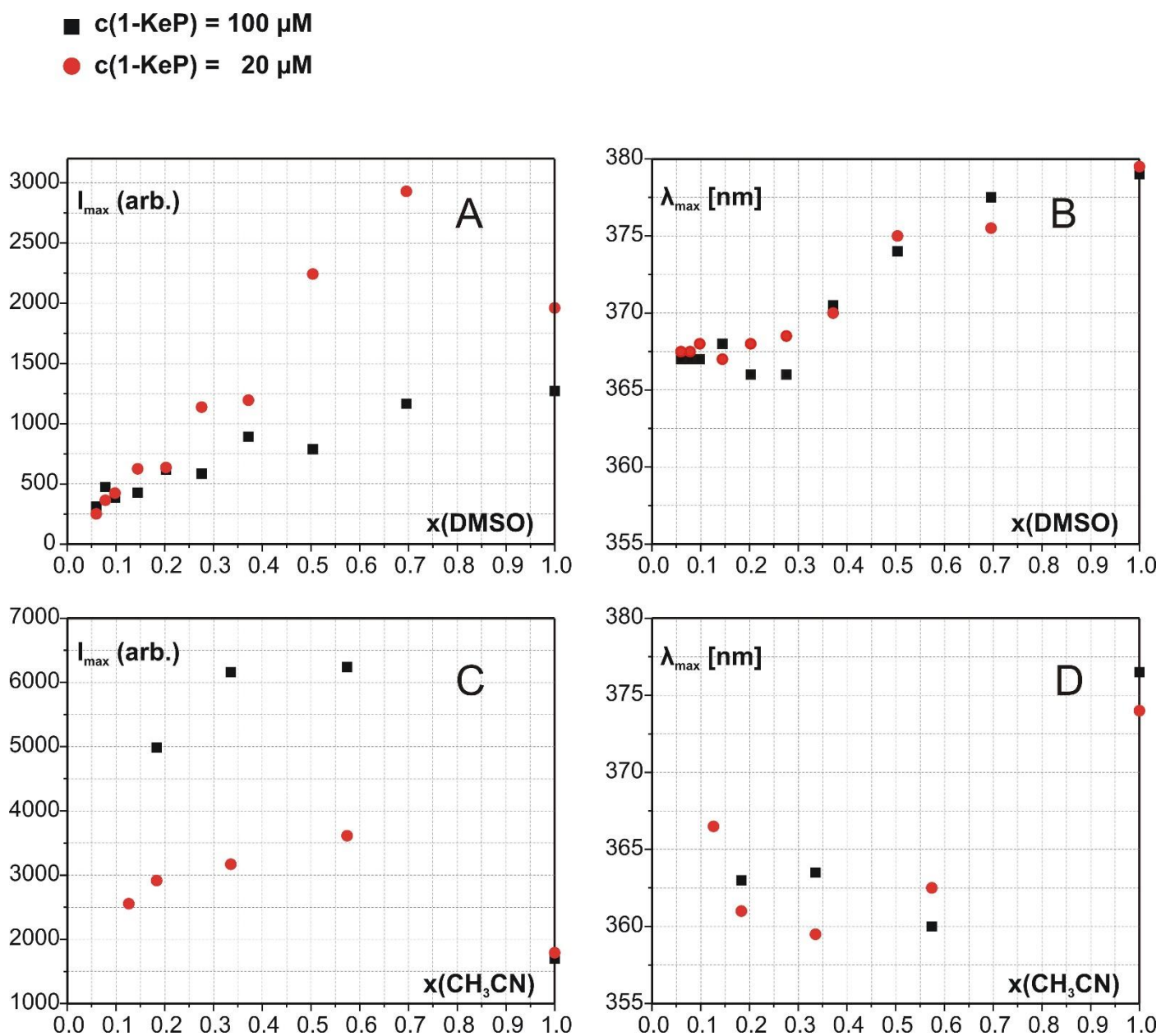


**Fig.S10.** Luminescence data for **1-KeP** in H<sub>2</sub>O+DMSO (A, B) and H<sub>2</sub>O+CH<sub>3</sub>CN (C, D) in two concentrations: 100  $\mu\text{M}$  (■black squares) and 20  $\mu\text{M}$  (●red circles). A, C: fluorescence intensity at the **Ke** fluorescence band maximum (excitation: 295 nm) B, D: position of the fluorescence band maximum (excitation: 295 nm) as function of the mole fraction of the organic solvent (DMSO or CH<sub>3</sub>CN).

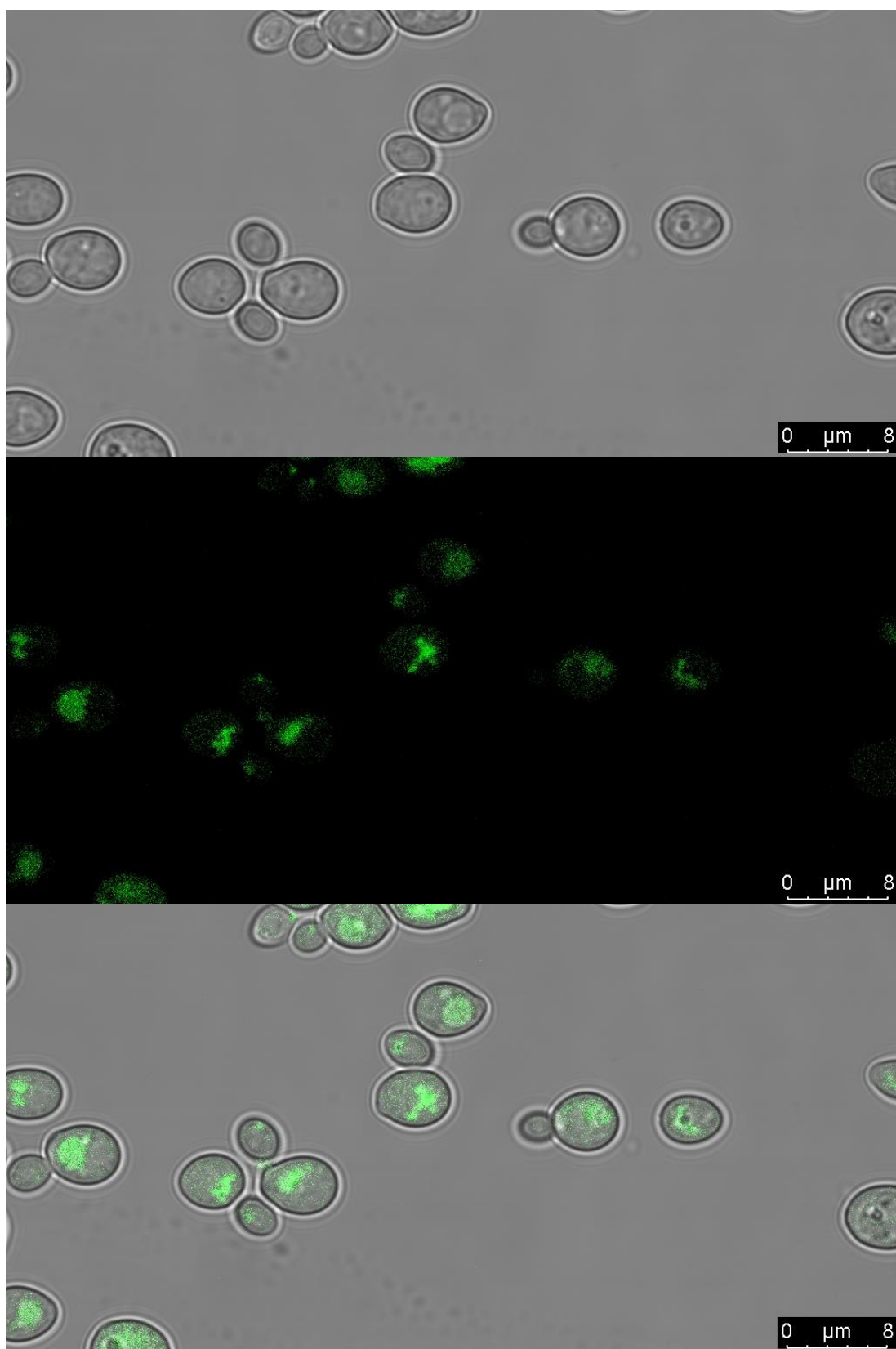


**Fig.S11-A.** Staining of the DSY1050 strain with **1-KeP** imaged by confocal microscopy (excitation at 405 nm, emission 600 - 700 nm signal collected). Top: bright field; Middle: luminescence; Bottom: merged.

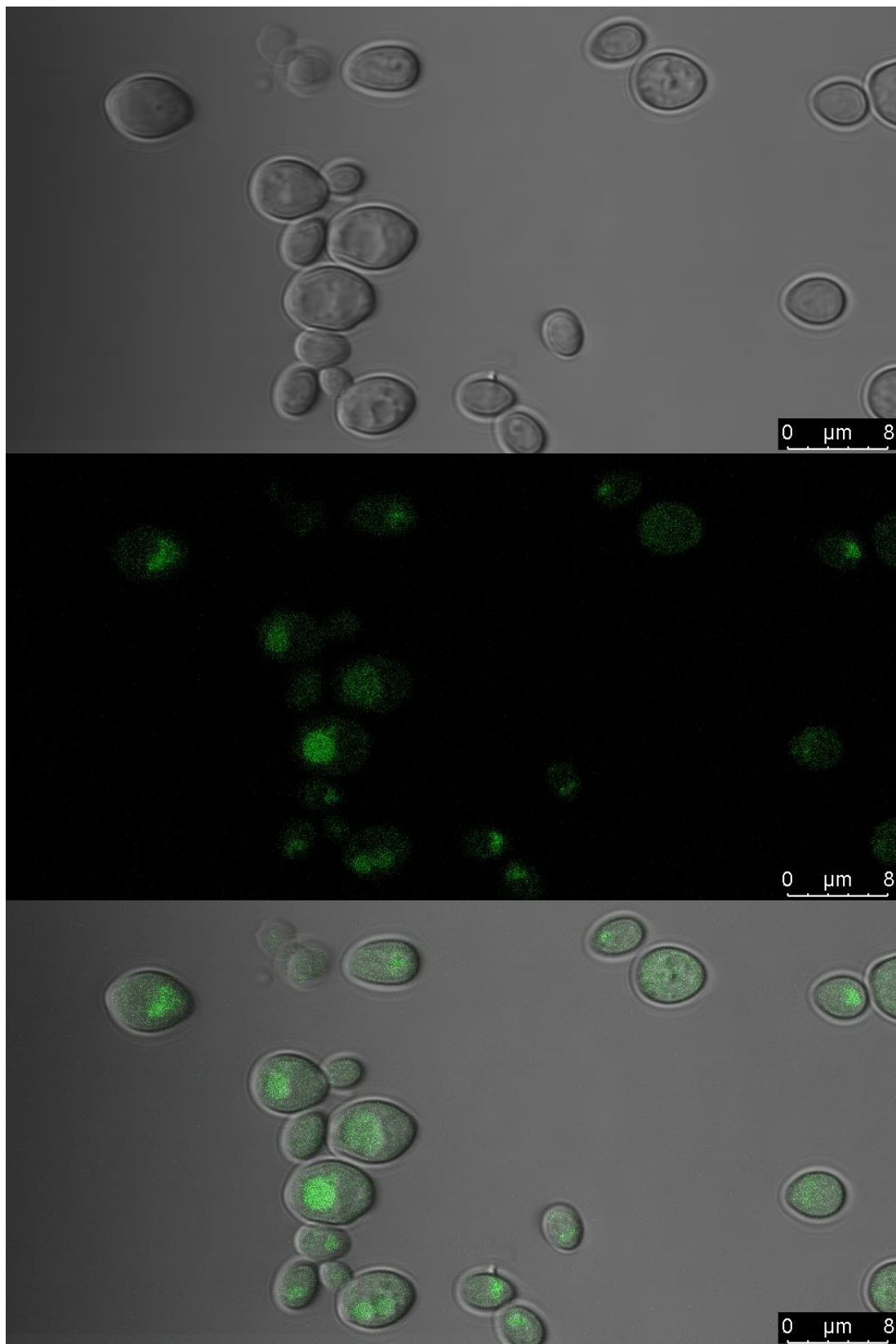


**Fig.S11-B.** Staining of the DSY1050 strain with **1-KeP** imaged by confocal microscopy (excitation at 405 nm, emission 600 - 700 nm signal collected). Top: bright field; Middle: luminescence; Bottom: merged.



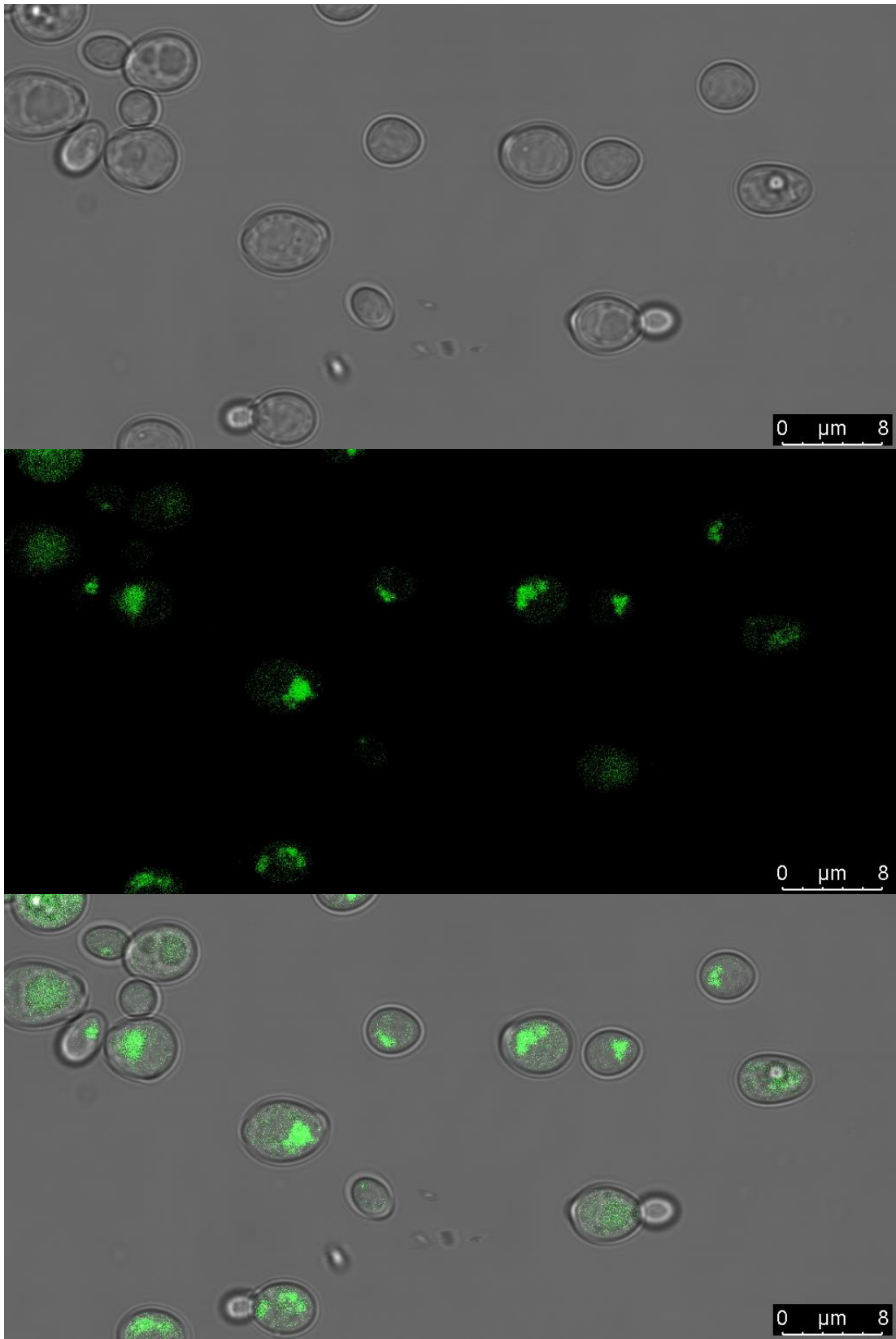


**Fig.S11-C.** Staining of the DSY1050 strain with **1-KeP** imaged by confocal microscopy (excitation at 405 nm, emission 600 - 700 nm signal collected). Top: bright field; Middle: luminescence; Bottom: merged.

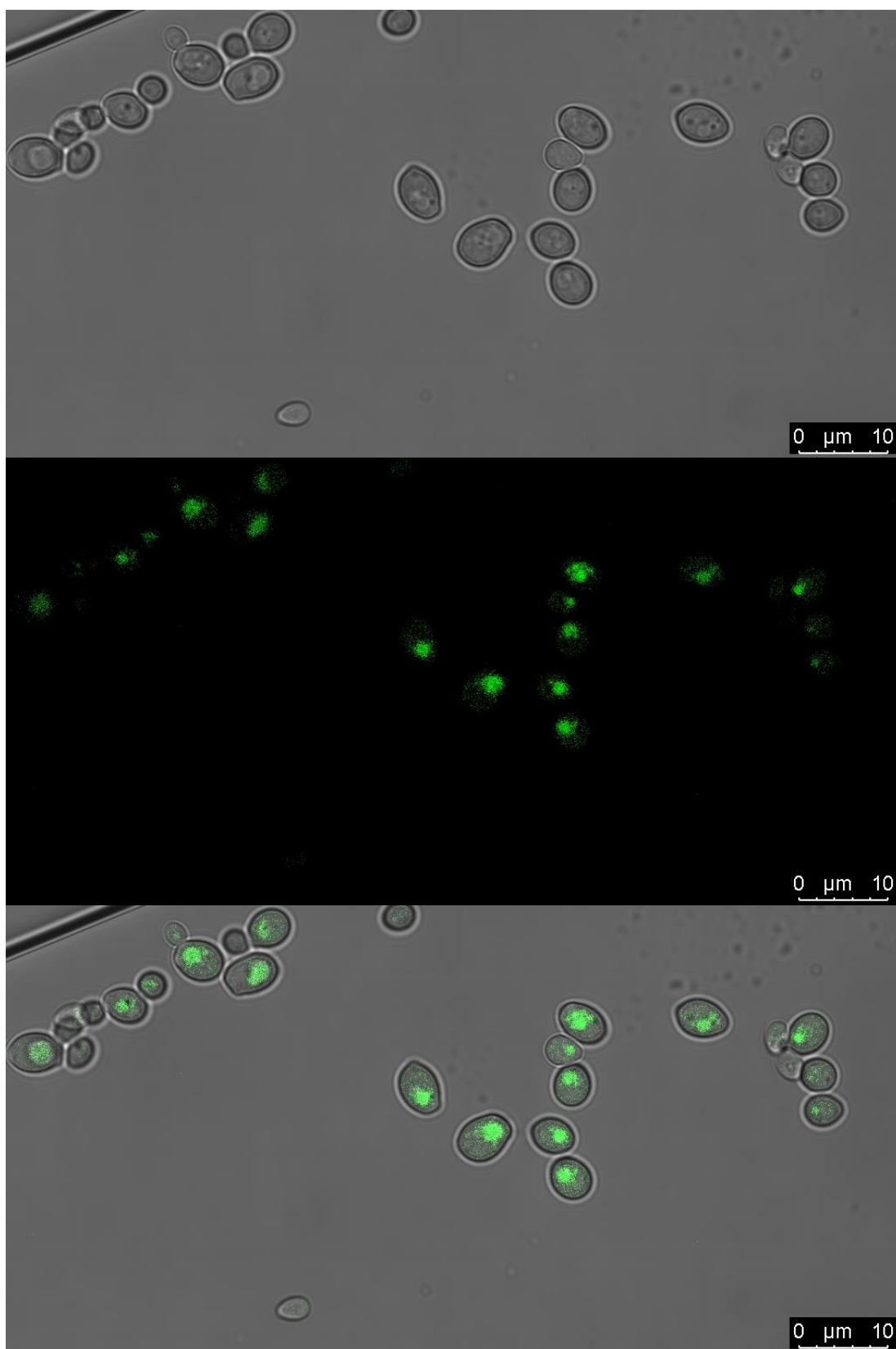


**Fig.S12-A.** Staining of the DSY1050 strain with **2-KeP** imaged by confocal microscopy (excitation at 405 nm, emission 600 - 700 nm signal collected). Top: bright field; Middle: luminescence; Bottom: merged.

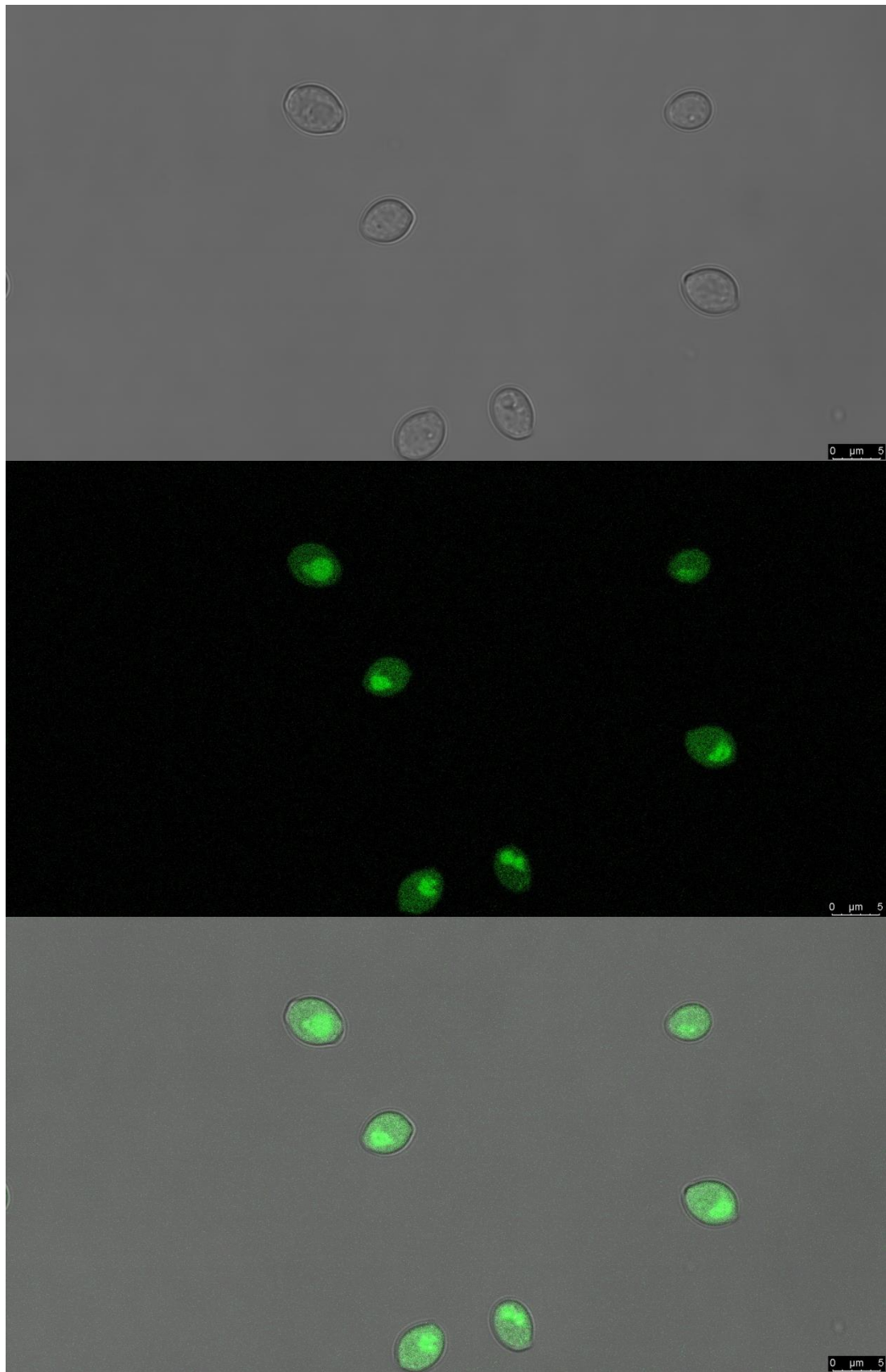


**Fig.S12-B.** Staining of the DSY1050 strain with **2-KeP** imaged by confocal microscopy (excitation at 405 nm, emission 600 - 700 nm signal collected). Top: bright field; Middle: luminescence; Bottom: merged.

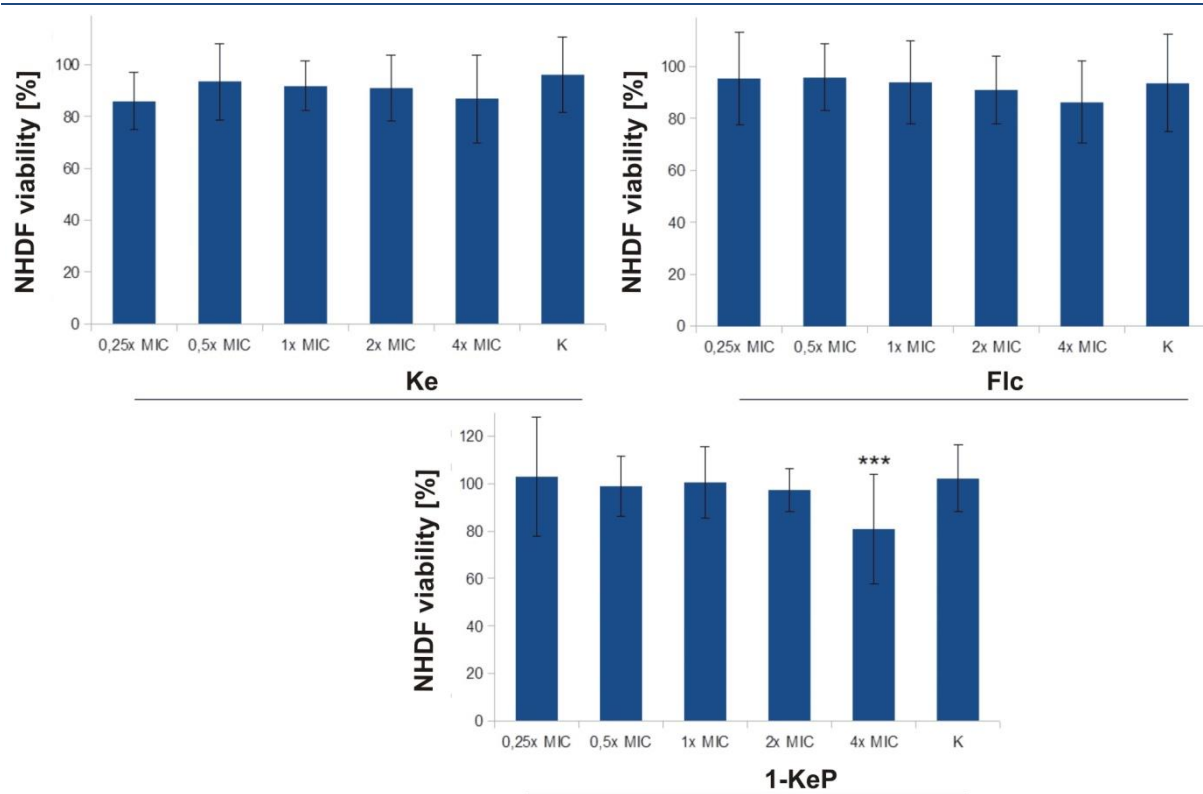


**Fig.S13** Proliferation rate of NHDF cells measured by MTT assay. NHDF cells were treated with 0.25; 0.5; 1; 2 and 4 x MIC<sub>50</sub> concentrations of **Ke**, **Flc** and **1-KeP** for 72 h, incubated with MTT and the number of viable cells measured spectrophotometrically at 540 nm. The bars represent the means  $\pm$  SD of triplicate values for three independent experiments. \*\*\*P<0.001.

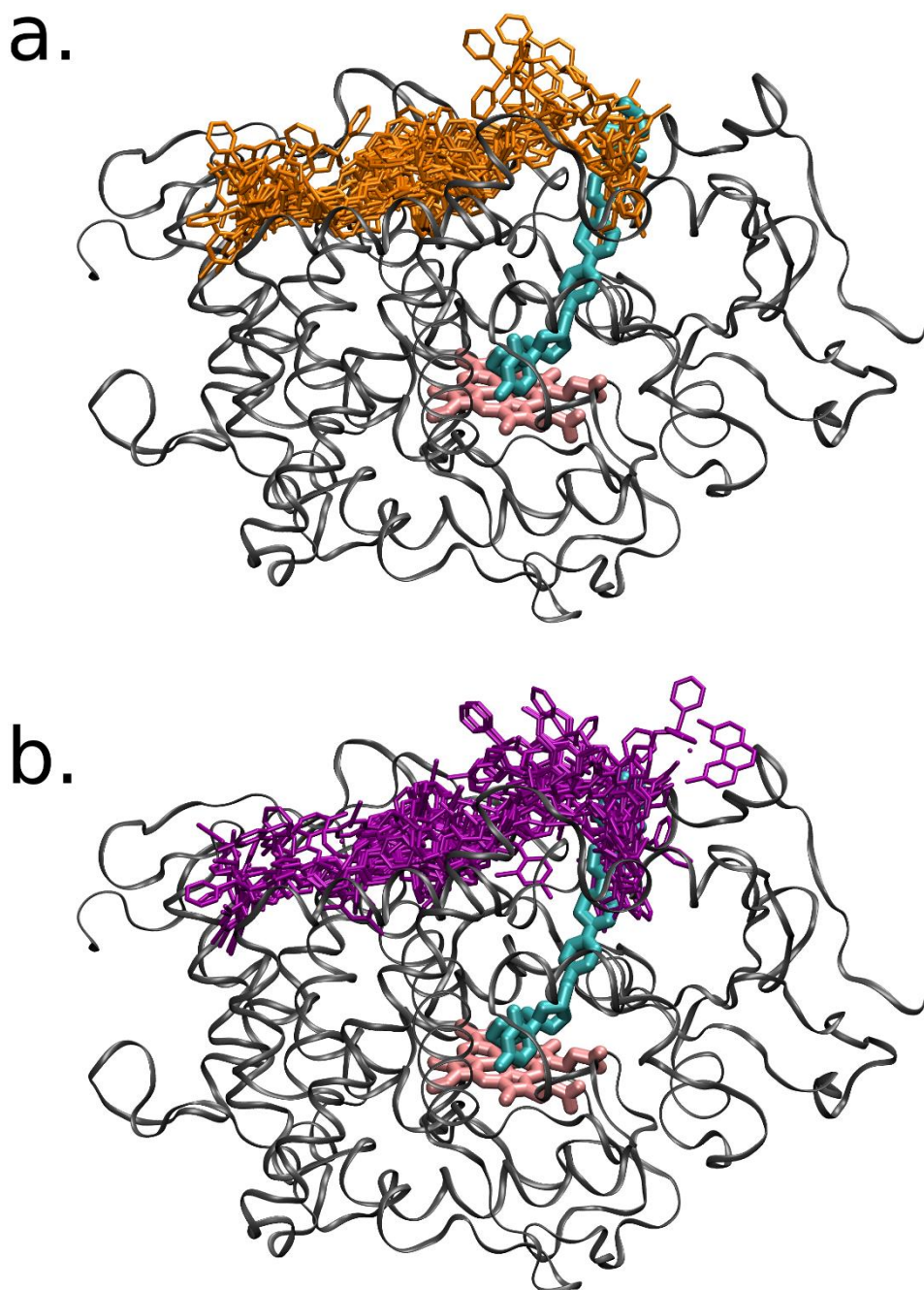


**Fig.S14** Docking of a) **1-KeP** (orange) and b) **2-KeP** (purple) to the CYP51 of *C. albicans* (grey ribbons). Experimental positions of the heme cofactor (pink) and the inhibitor – posaconazole (cyan) – are taken from the 5FSA PDB deposit. Docking ensembles of 27 conformations are shown for each ligand. The large molecules of the complexes **1-KeP** and **2-KeP** are not able to enter the binding cavity accessible to the posaconazole molecule; in particular, they are not able to interact directly with the heme cofactor. They are, instead, located on the protein surface, possibly obstructing the entrance to the binding cavity.

## REFERENCES

- 1 Eds. A. Casini, A. Vessières, S. M. Meier-Menches, Metal-based Anticancer Agents, Royal Society of Chemistry, **2019**, ISBN 978-1-78801-406-9 <https://doi.org/10.1039/9781788016452>
- 2 C. Santini, M. Pellei, V. Gandin, M. Porchia, F. Tisato, C. Marzano, Advances in Copper Complexes as Anticancer Agents, *Chem. Rev.*, 2014, **114**, 815-862 <https://doi.org/10.1021/cr400135x1uyh>
- 3 L. Colina-Vegas, W. Villarreal, M. Navarro, Copper(I)–phosphine complexes: a promising approach in the search for antitumor agents, Ed.: M. S. Balakrishna, Copper(I) Chemistry of Phosphines, Functionalized Phosphines and Phosphorus Heterocycles, Elsevier, 2019, 109-143, ISBN 9780128150528, <https://doi.org/10.1016/B978-0-12-815052-8.00005-1>
- 4 C., Marzano, F., Tisato, M., Porchia, M., Pellei, V. Gandin, Phosphine copper(I) complexes as anticancer agents: biological characterization. Part II, Ed.: M. S. Balakrishna, Copper(I) Chemistry of Phosphines, Functionalized Phosphines and Phosphorus Heterocycles Elsevier, **2019**, 83-107, ISBN 9780128150528, <https://doi.org/10.1016/B978-0-12-815052-8.00004-X>
- 5 Ed: L. Martinez, The evolving threat of antimicrobial resistance – Options for actions, World Health Organization, **2012**, ISBN 978-92-4-15031-1
- 6 M. C. Fisher, N. J. Hawkins, D. Sanglard, S. J. Gurr, Worldwide emergence of resistance to antifungal drugs challenges human health and food security., *Science*, 2018, **360**, 739-742 <https://doi.org/10.1126/science.aap7999>
- 7 L. Krishnasamy, S. Krishnakumar, G. Kumaramanickavel, C. Saikumar, Molecular mechanisms of antifungal drug resistance in Candida species., *J. Clin. Diagnostic Res.*, 2018, **12**, DE01–DE06 <https://doi.org/10.7860/JCDR/2018/36218.11961>
- 8 M. B., Lohse, M., Gulati, A. D., Johnson, C. J. Nobile, Development and regulation of single-and multi-species Candida albicans biofilms., *Nat. Rev. Microbiol.*, 2018, **16**, 19–31 <https://doi.org/10.1038/nrmicro.2017.107>
- 9 S. G. Whaley, E. L. Berkow, J. M. Rybak, A. T. Nishimoto, K. S. Barker, P. D. Rogers, Azole Antifungal Resistance in Candida albicans and Emerging Non-albicans Candida Species., *Front Microbiol.*, 2017, **12**, A2173 <https://doi.org/10.3389/fmicb.2016.02173>
- 10 K. T. Gunsalus, C. A. Kumamoto, Transcriptional Profiling of Candida albicans in the Host., *Methods Mol. Biol.*, 2016, **1356**, 17-29 [https://doi.org/10.1007/978-1-4939-3052-4\\_2](https://doi.org/10.1007/978-1-4939-3052-4_2)
- 11 T. P. Salci, M. Negri, A. K. R. Abadio, T. I. E. Svidzinski, É. S. Kioshima, Targeting Candida spp. to develop antifungal agents., *Drug Discov. Today*, 2018, **23**, 802–814 <https://doi.org/10.1016/j.drudis.2018.01.003>
- 12 L. Rodriguez, B. Bustamante, L. Huaroto, C. Agurto, R. Illescas, R. Ramirez, A. Diaz, J. Hidalgo, A multi-centric study of Candida bloodstream infection in Lima-Callao, Peru: species distribution, antifungal resistance and clinical outcomes. *PLoS One*, 2017, **12**, e0175172 <https://doi.org/10.1371/journal.pone.0175172>
- 13 A. Levina, D. C. Crans, P. A. Lay, Speciation of Metal Drugs, Supplements and Toxins in Media and Bodily Fluids Controls In-Vitro Activities, *Coord. Chem. Rev.* 2017, **352**, 473-498 <http://doi.org/10.1016/j.ccr.2017.01.002>
- 14 B N. Cioffi, L. Torsi, N. Ditaranto, G. Tantillo, L. Ghibelli, Luigia Sabbatini, Teresa Blevè-Zacheo, Maria D'Alessio, P. G. Zambonin, Enrico Traversa, Copper Nanoparticle/Polymer Composites with Antifungal and Bacteriostatic Properties, *Chem. Mater.* 2005, **17**, 5255-5262 <https://doi.org/10.1021/cm0505244>
- 15 Y. Wei, S. Chen, B. Kowalczyk, S. Huda, T. P. Gray, B. A. Grzybowski, Synthesis of Stable, Low-Dispersity Copper Nanoparticles and Nanorods and Their Antifungal and Catalytic Properties, *J. Phys. Chem. C* 2010, **114**, 15612–15616 <https://doi.org/10.1021/jp1055683>
- 16 M. E. Helsel, E. J. White, S. Z. A. Razvi, B. Alies, K. J. Franz, Chemical and functional properties of metal chelators that mobilize copper to elicit fungal killing of Cryptococcus neoformans, *Metallomics* 2017, **9**, 69–81. <https://doi.org/10.1039/c6mt00172f>
- 17 S. Shams, B. Ali, M. Afzal, I. Kazmi, F. A. Al-Abbasi, F. Anwar, Antifungal effect of Gatifloxacin and copper ions combination, *J. Antibiot.* 2014, **67**, 499–504 <https://doi.org/10.1038/ja.2014.35>

- 18 E. W. Hunsaker, K. J. Franz, Copper potentiates azole antifungal activity in a way that does not involve complex formation, *Dalton Trans.* 2019, **48**, 9654-9662 <https://doi.org/10.1039/C9DT00642G>
- 19 E. W. Hunsaker, K. J. Franz, *Candida albicans* reprioritizes metal handling during fluconazole stress, *Metallomics* 2019, **11**, 2020-2032 <https://doi.org/10.1039/C9MT00228F>
- 20 A. Bykowska, R. Starosta, J. Jezierska, M. Jeżowska-Bojczuk, Coordination versatility of phosphine derivatives of fluoroquinolones. New Cu<sup>I</sup> and Cu<sup>II</sup> complexes and their interactions with DNA., *RSC Advances*, 2015, **5**, 80804-80815 <https://doi.org/10.1039/c5ra07483e>
- 21 R. Starosta, U. K. Komarnicka, M. Puchalska, Luminescent copper(I) (pseudo)halide complexes with neocuproine and a novel bulky tris(aminomethyl)phosphine derived from 2-piperazinopyridine., *J. Lumin.*, 2013, **143**, 137-144 <https://doi.org/10.1016/j.jlumin.2013.04.050>
- 22 R. Starosta, U. K. Komarnicka, M. Puchalska, Solid state luminescence of CuI and CuNCS complexes with phenanthrolines and a new tris(aminomethyl)phosphine derived from N-methyl-2-phenylethanamine., *J. Lumin.*, 2014, **145**, 430-437 <https://doi.org/10.1016/j.jlumin.2013.07.015>
- 23 U. K. Komarnicka, R. Starosta, A. Kyzioł, M. Jeżowska-Bojczuk, Copper(I) complexes with phosphine derived from sparfloxacin. Part I – structures, spectroscopic properties and cytotoxicity., *Dalton Trans.*, 2015, **44**, 12688-12699 <https://doi.org/10.1039/c5dt01146a>
- 24 U. K. Komarnicka, R. Starosta, M. Płotek, R. F. M. de Almeida, M. Jeżowska-Bojczuk, A. Kyzioł, Copper(I) complexes with phosphine derived from sparfloxacin. Part II: a first insight into the cytotoxic action mode., *Dalton Trans.*, 2016, **45**, 5052-5063 <https://doi.org/10.1039/C5DT04011F>
- 25 V. Gandin, F. Tisato, A. Dolmella, M. Pellei, C. Santini, M. Giorgetti, C. Marzano, M. Porchia, In Vitro and in Vivo Anticancer Activity of Copper(I) Complexes with Homoscorpionate Tridentate Tris(pyrazolyl)borate and Auxiliary Monodentate Phosphine Ligands, *J. Med. Chem.* 2014, **57**, 4745-4760 <https://doi.org/10.1021/jm500279x>
- 26 U. K. Komarnicka, S. Kozioł, R. Starosta, A. Kyzioł, Selective Cu(II) complex with phosphine-peptide (SarGly) conjugate contra breast cancer: synthesis, spectroscopic characterization and insight into cytotoxic action, *J. Inorg. Biochem.* 2018, **186**, 162-175 <https://doi.org/10.1016/j.jinorgbio.2018.06.009>
- 27 M Patra, T. Joshi, V. Pierroz, K. Ingram, M. Kaiser, S. Ferrari, B. Spingler, J. Keiser, G. Gasser, DMSO-Mediated Ligand Dissociation: Renaissance for Biological Activity of N-Heterocyclic-[Ru( $\eta^6$ -arene)Cl<sub>2</sub>] Drug Candidates, *Chem. Eur. J.* 2013, **19**, 14768-14772 <https://doi.org/10.1002/chem.201303341>
- 28 A. Kobayashi, K. Komatsu, H. Ohara, W. Kamada, Y. Chishina, K. Tsuge, H.-C. Chang, M. Kato, Photo- and Vapor-Controlled Luminescence of Rhombic Dicopper(I) Complexes Containing Dimethyl Sulfoxide, *Inorg. Chem.* 2013, **52**, 13188–13198 <https://doi.org/10.1021/ic402104q>
- 29 V. Patel, B. Liaw, W. Oh, The role of ketoconazole in current prostate cancer care., *Nature Rev. Urol.*, 2018, **15**, 643–651 <https://doi.org/10.1038/s41585-018-0077-y>
- 30 P. Contreras, E. Altieri, C. Liberman, A. Gac, A. Rojas, A. Ibarra, M. Ravanal, M. Seron-Ferre, Adrenal rest tumor of the liver causing Cushing's syndrome: treatment with ketoconazole preceding an apparent surgical cure., *J. Clin. Endocrinol. Metab.*, 1985, **60**, 21-28 <https://doi.org/10.1210/jcem-60-1-21>
- 31 Committee for Medicinal Products for Human Use (CHMP), Assessment report Ketoconazole HRA, Procedure No. EMEA/H/C/003906/0000 [https://www.ema.europa.eu/documents/assessment-report/ketoconazole-hra-epar-public-assessment-report\\_en.pdf](https://www.ema.europa.eu/documents/assessment-report/ketoconazole-hra-epar-public-assessment-report_en.pdf) (accessed Mar. 20. 2020)
- 32 B. C. Das, A. V. Madhukumar, J. Anguiano, S. Kim, M., Sinz, T. A. Zvyaga, E. C. Power, C. R. Ganellin, S. Mani, Synthesis of novel ketoconazole derivatives as inhibitors of the human Pregnane X Receptor (PXR, NR1I2, also termed SXR, PAR)., *Bioorg. Med. Chem. Lett.*, 2008, **18**, 3974-3977 <https://doi.org/10.1016/j.bmcl.2008.06.018>
- 33 S. ManiBhasar, C. Das, Ketoconazole-derivative antagonists of human pregnane x receptor. U.S. Patent 8669260, **2011**

- 34 P. Pirson, B. Leclef, A. Trouet, Activity of ketoconazole derivatives against *Leishmania mexicana amazonensis* within mouse peritoneal macrophages., *Ann. Trop. Med. Parasitol.*, 1990, **84**, 133-139 <https://doi.org/10.1080/00034983.1990.11812446>
- 35 M. S. Rieber, A. Anzellotti, R. A. Sánchez-Delgado, M. Rieber, Tumor apoptosis induced by ruthenium(II)-ketoconazole is enhanced in nonsusceptible carcinoma by monoclonal antibody to EGF receptor., *Int. J. Cancer*, 2004, **112**, 376–384 <https://doi.org/10.1002/ijc.20415>
- 36 E. Robles-Escajeda, A. Martínez, A. Varela-Ramirez, R. A. Sánchez-Delgado, R. J. Aguilera, Analysis of the cytotoxic effects of ruthenium – ketoconazole and ruthenium – clotrimazole complexes on cancer cells., *Cell Biol. Toxic.*, 2013, **29**, 431-443 <https://doi.org/10.1007/s10565-013-9264-z>
- 37 T. Gagini, L. Colina-Vegas, W. Villarreal, L. P. Borba-Santos, P. C. de Souza, A. A. Batista, F. M. Kneip, W. de Souza, S. Rozental, L. A. S. Costa, M. Navarro, Metal–azole fungistatic drug complexes as anti-Sporothrix spp. Agents., *New J. Chem.*, 2018, **42**, 13641-13650 <https://doi.org/10.1039/C8NJ01544A>
- 38 R. F. M. de Almeida, F. C. Santos, K. Marycz, M. Alicka, A. Krasowska, J. Suchodolski, J. J. Panek, A. Jezierska, R. Starosta, New diphenylphosphane derivatives of ketoconazole are promising antifungal agents., *Sci. Rep.*, 2019, **9**, 16214 <https://doi.org/10.1038/s41598-019-52525-7>
- 39 D. S. Loose, P. B. Kan, M. A. Hirst, R. A. Marcus, D. Feldman, Ketoconazole blocks adrenal steroidogenesis by inhibiting cytochrome P450-dependent enzymes., *J. Clin. Invest.*, 1983, **71**, 1495–1499 <https://doi.org/10.1172/JCI110903>
- 40 A. Bykowska, R. Starosta, A. Brzuskiewicz, B. Bażanów, M. Florek, N. Jackulak, J. Król, J. Grzesiak, K. Kaliński, M. Jeżowska-Bojczuk, Synthesis, properties and biological activity of a novel phosphine ligand derived from ciprofloxacin., *Polyhedron*, 2013, **60**, 23-29 <https://doi.org/10.1016/j.poly.2013.04.059>
- 41 A. Bykowska, R. Starosta, U. K. Komarnicka, Z. Ciunik, A. Kyzioł, K. Guz-Regner, G., Bugła-Płoskońska, M. Jeżowska-Bojczuk, Phosphine derivatives of ciprofloxacin and norfloxacin, a new class of potential therapeutic agents., *New J. Chem.*, 2014 **38**, 1062-1071 <https://doi.org/10.1039/c3nj01243c>
- 42 U. K. Komarnicka, R. Starosta, A. Kyzioł, M. Płotek, M. Puchalska, M. Jeżowska-Bojczuk, New copper(I) complexes bearing lomefloxacin motif: spectroscopic properties, in vitro cytotoxicity and interactions with DNA and human serum albumin., *J. Inorg. Biochem.*, 2016, **165**, 25-35 <https://doi.org/10.1016/j.jinorgbio.2016.09.015>
- 43 B. R. James, R. J. P. Williams, 383. The oxidation–reduction potentials of some copper complexes, *J. Chem. Soc.* **1961**, 2007-2019 <https://doi.org/10.1039/JR9610002007>
- 44 C. E. McCusker, F. N. Castellano, Design of a Long-Lifetime, Earth-Abundant, Aqueous Compatible Cu(I) Photosensitizer Using Cooperative Steric Effects, *Inorg. Chem.* 2013, **52**, 8114-8120 <https://doi.org/10.1021/ic401213p>
- 45 R. Starosta, A. Bykowska, A. Kyzioł, M. Płotek, M. Florek, J. Król, M. Jeżowska-Bojczuk, Copper(I) (pseudo)halide complexes with neocuproine and aminomethylphosphines derived from morpholine and thiomorpholine - in vitro cytotoxic and antimicrobial activity and the interactions with DNA and serum albumins., *Chem. Biol. Drug Des.*, 2013, **82**, 579-586 <https://doi.org/10.1111/cbdd.12187>
- 46 R. Starosta, M. Puchalska, J. Cybińska, M. Barys, A. V. Mudring, Structures, electronic properties and solid state luminescence of Cu(I) iodide complexes with 2,9-dimethyl-1,10-phenanthroline and aliphatic aminomethylphosphines or triphenylphosphine., *Dalton Trans.*, 2011, **40**, 2459-2468 <https://doi.org/10.1039/c0dt01284j>
- 47 R. Starosta, U. K. Komarnicka, M. Puchalska, M. Barys, Solid state luminescence of copper(I) (pseudo)halide complexes with neocuproine and aminomethylphosphanes derived from morpholine and thiomorpholine., *New J. Chem.*, 2012, **36**, 1673-1683 <https://doi.org/10.1039/C2NJ40229G>
- 48 F. Jalali, A. Afshoon, Spectrofluorimetric Study and Detection of Ketoconazole in the Presence of  $\beta$ -cyclodextrin., *J. Fluoresc.*, 2008, **18**, 219–225 <https://doi.org/10.1007/s10895-007-0265-2>
- 49 F. Jalali, A. Afshoon, M. Shamsipur, Micellar-enhanced spectrofluorimetric determination of ketoconazole in cetyltrimethylammonium bromide medium. *Chem Anal.* 2007, **52**, 115–123 EID: 2-s2.0-34047274959



- 50 P. Y. Khashaba, K. M. Emara, A. M. Mohamed, Analysis of some antifungal drugs by spectrophotometric and spectrofluorimetric methods in different pharmaceutical dosage forms., *J. Pharm. Biomed. Anal.*, 2000, **22**, 363–376 [https://doi.org/10.1016/S0731-7085\(99\)00280-0](https://doi.org/10.1016/S0731-7085(99)00280-0)
- 51 A. El-Bayoumi, A. A. El-Shanawany, M. E. El-Sadek, A. Abd-ElSattar, Synchronous spectrofluorimetric determination of famotidine, fluconazole and ketoconazole in bulk powder and in pharmaceutical dosage forms., *Spect. Lett.*, 1997, **30**, 25–46 <https://doi.org/10.1080/00387019708002587>
- 52 R. Starosta, R.F.M. de Almeida, Luminescence properties of the antifungal agent ketoconazole and its diphenylphosphane derivatives, *J. Lumin.*, 2020, **220**, 116956 <https://doi.org/10.1016/j.jlumin.2019.116956>
- 53 B. Kobin, L. Grubert, S. Blumstengel, F. Henneberger, S. Hecht., Vacuum-Processable Ladder-type Oligophenylenes for Organic-Inorganic Hybrid structures: Synthesis, Optical and Electrochemical Properties upon Increasing Planarization as Well as Thin Film Growth., *J. Mat. Chem.*, 2012, **22**, 4383–4390 <http://doi.org/10.1039/C2JM15868J>
- 54 Z. Lu, E. Manias, D. D. Macdonald, M. Lanagan, Dielectric Relaxation in Dimethyl Sulfoxide/Water Mixtures Studied by Microwave Dielectric Relaxation Spectroscopy., *J. Phys. Chem. A*, 2009, **113**, 12207–12214 <https://doi.org/10.1021/jp9059246>
- 55 R. Jellema, J. Bulthuis, G. van der Zwan, Dielectric relaxation of acetonitrile-water mixtures. *J. Mol. Liquids*, 1997, **73–74**, 179-193 [https://doi.org/10.1016/S0167-7322\(97\)00066-4](https://doi.org/10.1016/S0167-7322(97)00066-4)
- 56 J.,Suchodolski, J. Muraszko, P. Bernat, A. Krasowska, A Crucial Role for Ergosterol in Plasma Membrane Composition, Localisation, and Activity of Cdr1p and H<sup>+</sup>-ATPase in *Candida albicans*., *Microorganisms*, 2019, **7**, 378 <https://doi.org/10.3390/microorganisms7100378>
- 57 T. Y. Hargrove, L. Friggeri, Z. Wawrzak, A. Qi, W. J. Hoekstra, R. J. Schotzinger, J. D. York, F. P. Guengerich, G. I. Lepesheva, Structural analyses of *Candida albicans* sterol 14 $\alpha$ -demethylase complexed with azole drugs address the molecular basis of azole-mediated inhibition of fungal sterol biosynthesis., *J. Biol. Chem.*, 2017, **292**, 6728–6743 <https://doi.org/10.1074/jbc.M117.778308>
- 58 A. Krasowska, L. Chmielewska, J. Łuczyński, S. Witek, K. Sigler, Dual mechanism of the antifungal effect of new lysosomotropic agents on *Saccharomyces cerevisiae* RXII strain, *Cell. Mol. Biol. Lett.*, 2003, **8**, 111-120.
- 59 A. Krasowska, L. Chmielewska, R. Adamski, J. Łuczyński, S. Witek, K. Sigler, The sensitivity of yeast and yeast-like cells to new lysosomotropic agents, *Cell. Mol. Biol. Lett.*, 2004, **9**, 675–683.
- 60 C. De Duve, T. De Barsey, B. Poole, A. Trout, P. Tulkens, F. Van Hoff, Lysosomotropic agents., *Biochem. Pharmacol.*, 1974, **23**, 2495-2519 [https://doi.org/10.1016/0006-2952\(74\)90174-9](https://doi.org/10.1016/0006-2952(74)90174-9)
- 61 Gaussian 16, Revision B.01, M. J. Frisch et al., Gaussian, Inc., Wallingford CT, 2016.
- 62 J.-D. Chai, M. Head-Gordon, Long-range corrected hybrid density functionals with damped atom-atom dispersion corrections, *Phys. Chem. Chem. Phys.*, 2008, **10**, 6615-6620 <https://doi.org/10.1016/10.1039/B810189B>
- 63 K. L. Schuchardt, B. T. Didier, T. Elsethagen, L. Sun, V. Gurumoorthi, J. Chase, J. Li, T. L. Windus, Basis Set Exchange: A Community Database for Computational Sciences, *J. Chem. Inf. Model.*, 2007, **47**, 1045-1052 <https://doi.org/10.1021/ci600510j>
- 64 M. N. Glukhovtsev, A. Pross, M. P. McGrath, L. Radom, Extension of Gaussian-2 (G2) theory to bromine- and iodine-containing molecules: Use of effective core potentials, *J. Chem. Phys.*, 1995, **103**, 1878-1885 <https://doi.org/10.1063/1.469712>
- 65 G. M. Morris, R. Huey, W. Lindstrom, M. F. Sanner, R. K. Belew, D. S. Goodsell, A. J. Olson, AutoDock4 and AutoDockTools4: automated docking with selective receptor flexibility., *J. Comput. Chem.*, 2009, **16**, 2785-2791 <https://doi.org/10.1002/jcc.21256>
- 66 O. Trott, A. J. Olson, AutoDock Vina: improving the speed and accuracy of docking with a new scoring function, efficient optimization and multithreading., *J. Comput. Chem.*, 2010, **31**, 455-461 <https://doi.org/10.1002/jcc.21334>
- 67 W. Humphrey, A. Dalke, K. Schulten, VMD – Visual Molecular Dynamics., *J. Molec. Graph.*, 1996, **14**, 33–38 [https://doi.org/10.1016/0263-7855\(96\)00018-5](https://doi.org/10.1016/0263-7855(96)00018-5)

- 68 W. Fonzi, M. Irwin, Isogenic strain construction and gene mapping in *Candida albicans*., *Genetics*, 1993, **134**, 717–728 <https://doi.org/10.1046/j.1439-0507.1999.00498.x>
- 69 P. Mukherjee, J. Chandra, Mechanism of fluconazole resistance in *Candida albicans* biofilms: phase-specific role of efflux pumps and membrane sterols., *Infect. Immun.*, 2003, **71**, 4333–4340 <https://doi.org/10.1128/IAI.71.8.4333-4340.2003>
- 70 D. Sanglard, K. Kuchler, F. Ischer, J. L. Pagani, M. Monod, J. Bille, Mechanisms of resistance to azole antifungal agents in *Candida albicans* isolates from AIDS patients involve specific multidrug transporters., *Antimicrob. Agents Chemother.*, 1995, **39**, 2378–2386 <https://doi.org/10.1128/AAC.39.11.2378>
- 71 D. Sanglard, F. Ischer, Susceptibilities of *Candida albicans* multidrug transporter mutants to various antifungal agents and other metabolic inhibitors., *Antimicrob. Agents Chemother.*, 1996, **40**, 2300–2305 <https://doi.org/10.1128/AAC.40.10.2300>
- 72 R. Franz, M. Ruhnke J., Morschhäuser Molecular aspects of fluconazole resistance development in *Candida albicans*, *Mycoses*, 1999, **42**, 453-458 <https://doi.org/10.1046/j.1439-0507.1999.00498.x>
- 73 R. Wakieć, R. Prasad, J. Morschhäuser, F. Barchiesi, E. Borowski, S. Milewski, Voriconazole and multidrug resistance in *Candida albicans*., *Mycoses*, 2007, **50**, 109-115 <https://doi.org/10.1111/j.1439-0507.2006.01327.x>
- 74 Reference method for broth dilution antifungal susceptibility testing of yeast. Approved Standard, 3rd ed. M27-A3 28. Clinical and Laboratory Standards Institute, Wayne, PA. 2008 ISBN 1-56238-666-2
- 75 J. Suchodolski, A. Krasowska, Plasma Membrane Potential of *Candida albicans* Measured by Di-4-ANEPPS Fluorescence Depends on Growth Phase and Regulatory Factors., *Microorganisms*, 2019, **7**, 110 <https://doi.org/10.3390/microorganisms7040110>